Quantum quantum information and thermodynamics with ions

- Introduction to ion trapping and cooling
- Trapped ions as qubits for quantum computing and simulation
- Qubit architectures for scalable entanglement
- Quantum thermodynamics introduction
- Heat transport, Fluctuation theorems,
- Phase transitions, Heat engines
- Outlook

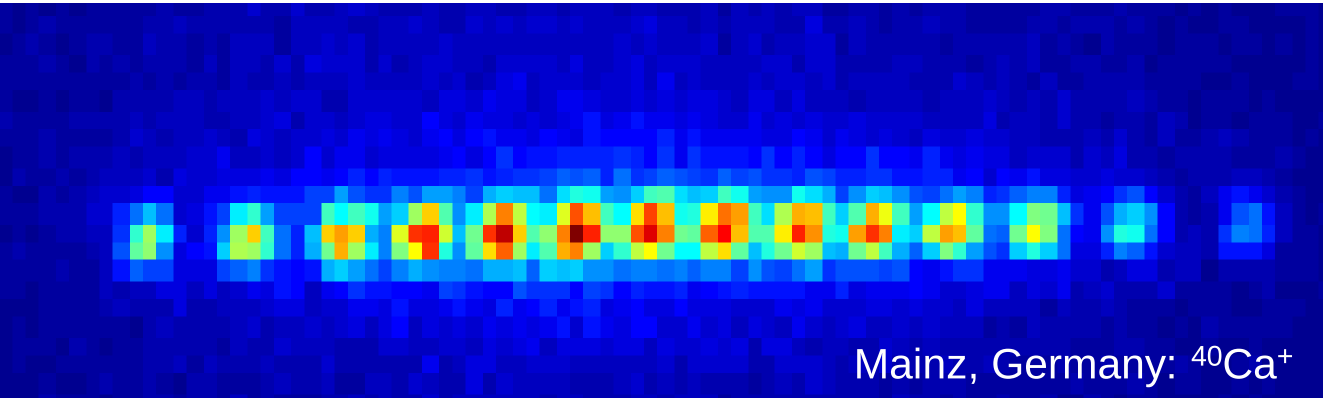

www.quantenbit.de

F. Schmidt-Kaler

JOHANNES GUTENBERG UNIVERSITÄT MAINZ

Ion Gallery

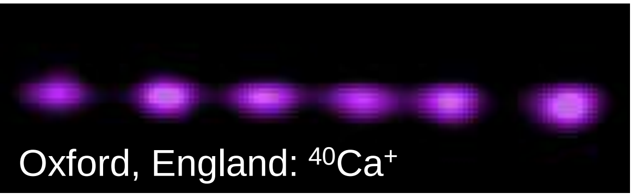

Oxford, England: $^{40}Ca^{+}$

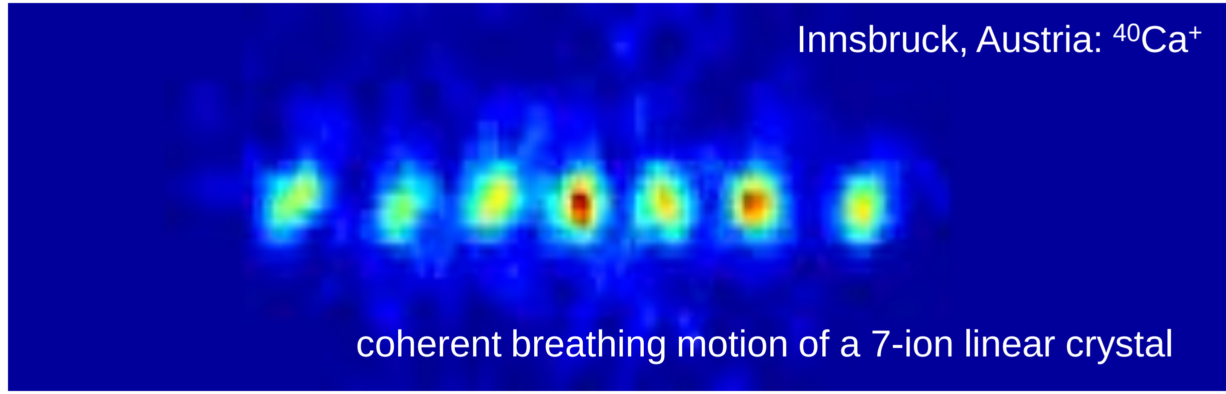

Innsbruck, Austria: $^{40}Ca^{+}$

coherent breathing motion of a 7-ion linear crystal

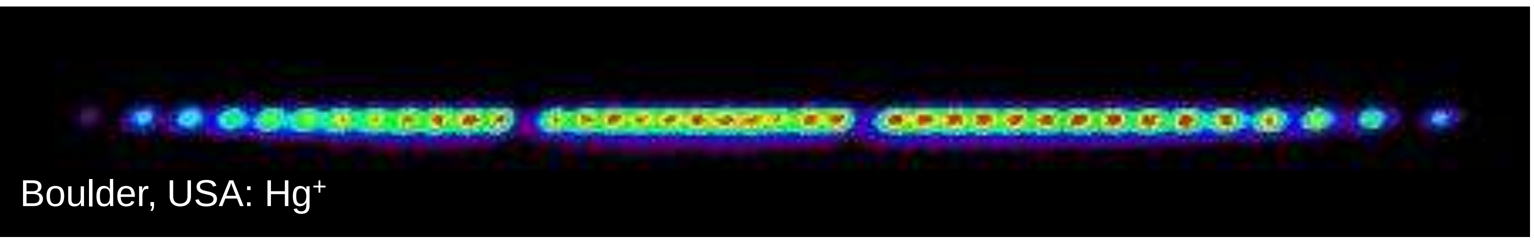

Boulder, USA: Hg^{+}

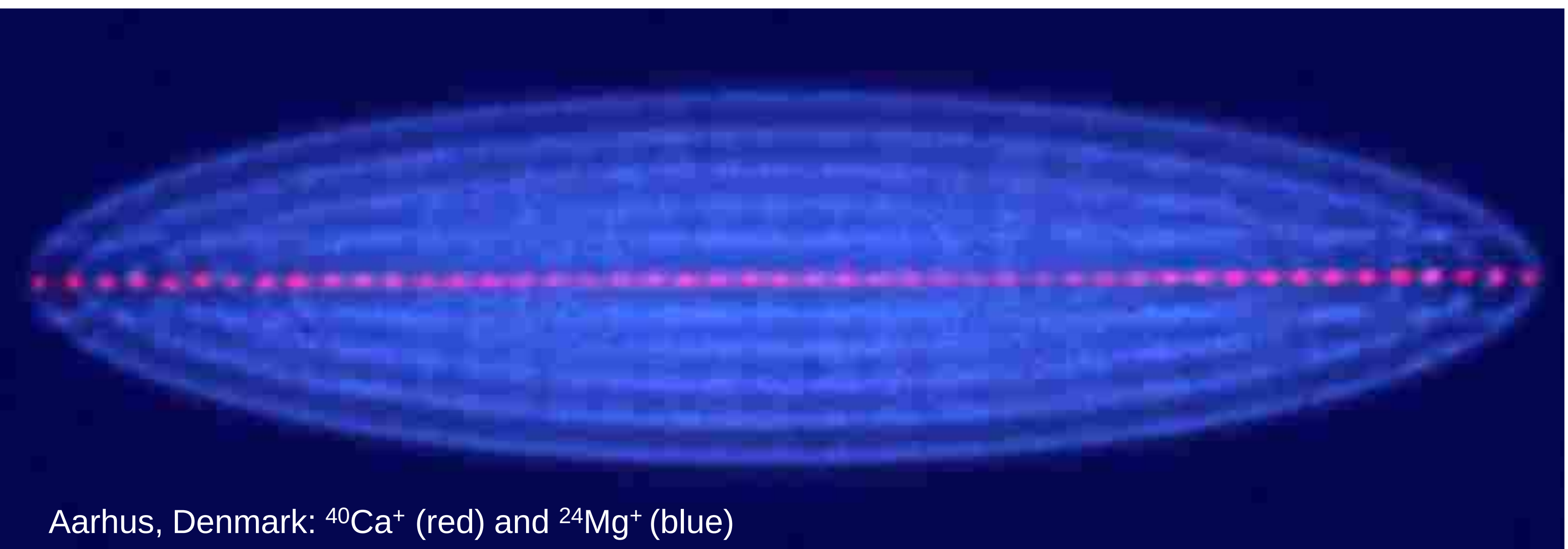

Aarhus, Denmark: $^{40}Ca^{+}$ (red) and $^{24}Mg^{+}$ (blue)

Why using ions?

- Ions in Paul traps were the first sample with which laser cooling was demonstrated and quite some Nobel prizes involve laser cooling…

- A single laser cooled ion still represents one of the best understood objects for fundamental investigations of the interaction between matter and radiation

- Experiments with single ions spurred the development of similar methods with neutral atoms and solid state physics

- Particular advantages of ions are that they are
  - confined to a very small spatial region ($\delta x < \lambda$)
  - controlled and measured at will for experimental times of days
  - strong, long-range coupling

- Ideal test ground for fundamental experiments

- Further applications for
  - precision measurements
  - thermodynamics with small systems
  - cavity QED
  - quantum sensors
  - quantum computing
  - quantum phase transitions
  - optical clocks
  - exotic matter

Introduction to ion trapping

- Paul trap
- Ion crystals
- Eigenmodes of a linear ion crystal
- Non-harmonic contributions

Modern segmented micro Paul trap

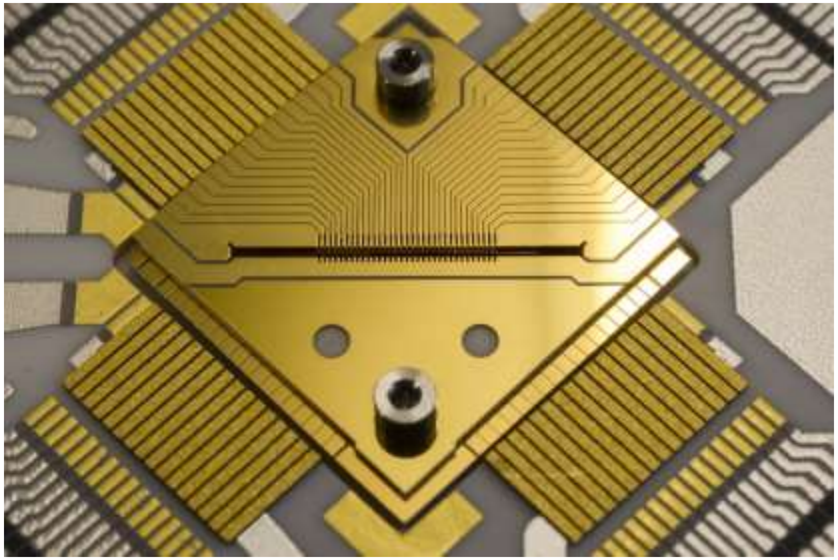

Traditional Paul trap

Dynamic confinement in a Paul trap

Invention of the Paul trap

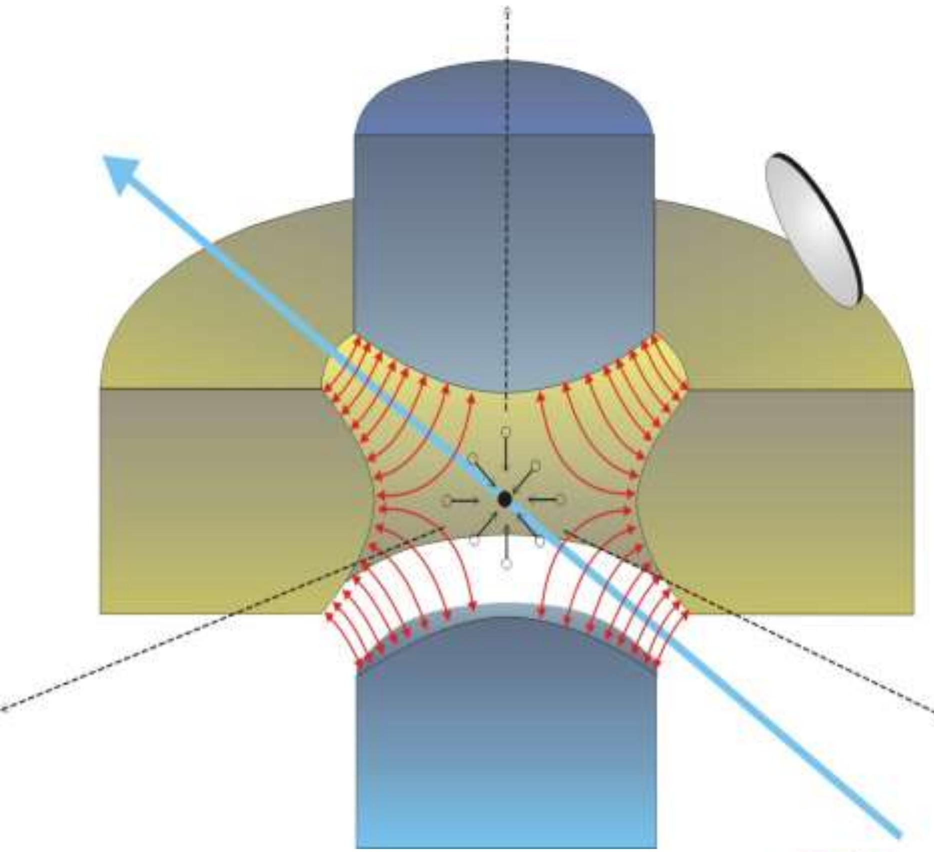

Wolfgang Paul (Nobel prize 1989)

DK 537.534.3 535.336.2

FORSCHUNGSBERICHTE
DES WIRTSCHAFTS- UND VERKEHRSMINISTERIUMS
NORDRHEIN-WESTFALEN

Herausgegeben von Staatssekretär Prof. Dr. h. c. Dr. E. h. Leo Brandt

Nr. 415

Prof. Dr.-Ing. Wolfgang Paul
Dr. rer. nat. Otto Osberghaus
Dipl.-Phys. Erhardt Fischer
Physikalisches Institut der Universität Bonn

Ein Ionenkäfig

Als Manuskript gedruckt

WESTDEUTSCHER VERLAG / KÖLN UND OPLADEN
1958

Binding in three dimensions

Electrical quadrupole potential $\Phi(\vec{r}) = \Phi_0 \cdot \sum \alpha_i (r_i/\tilde{r})^2, \quad i = x, y, z$

trap size: $\tilde{r}$

Binding force for charge *Q* $\vec{F}(\vec{r}) = Q\vec{E}(\vec{r}) = -Q\vec{\nabla}\Phi$

leads to a harmonic binding: $\vec{F}(\vec{r}) \sim \vec{r}$

Ion confinement requires a focusing force in 3 dimensions, but

Laplace equation requires $\vec{\nabla}^2\Phi = (\partial^2/\partial x^2 + \partial^2/\partial y^2 + \partial^2/\partial z^2)\Phi = 0$

such that at least one of the coefficients α_i is negative,
e.g. binding in x- and y-direction but anti-binding in z-direction !

no static trapping in 3 dimensions

Dynamical trapping: Paul's idea

time depending potential $\Phi(\vec{r}, t) = \Phi_0(t) \cdot (x^2 + y^2 - 2z^2)$

with $\Phi_0(t) = (U + V cos(\Omega_{RF} t))/\tilde{r}^2$

leads to the equation of motion for a particle with charge *Q* and mass *m*

$$\ddot{r}_i + \frac{2\alpha_i Q}{m r_0^2} \; \frac{U + V cos(\Omega_{RF} t)}{\tilde{r}^2} \; r_i = 0, \; \alpha_{x,y} = 1, \alpha_z = 2,$$

takes the standard form of the *Mathieu* equation
(linear differential equ. with time depending cofficients)

$$\boxed{\frac{d^2 u}{d\tau^2} + (a + 2\, q\; cos(2\tau))u = 0}$$

with substitutions

$$a_z = -2a_r = -\frac{8QU}{m\tilde{r}^2 \Omega_{RF}^2} \qquad q_z = -2q_r = -\frac{4QV}{m\tilde{r}^2 \Omega_{RF}^2}$$

radial and axial trap radius $\tilde{r}^2 = r_0^2 + 2z_0^2$ $\qquad \tau = \frac{1}{2}\Omega_{RF} t$

Theodor Hänsch‘s video
celebrating Wolfgang Paul invention

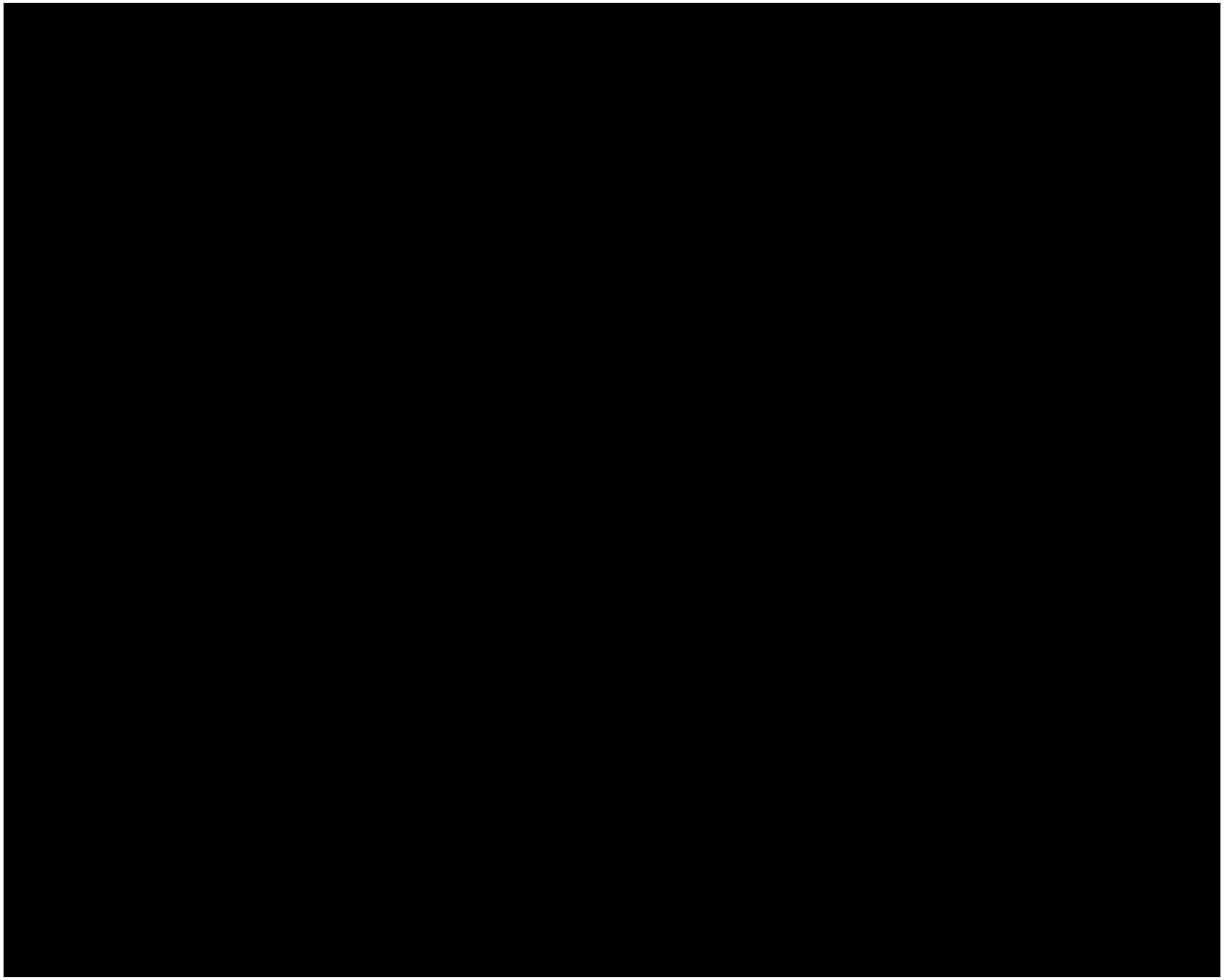

Regions of stability

time-periodic diff. equation leads to Floquet Ansatz

$$x(\tau) = Ae^{+i\mu\tau}\,\phi(\tau) + Be^{-i\mu\tau}\,\phi(\tau), \qquad \phi(\tau) = \phi(\tau+\pi) = \sum c_n e^{2in\tau}$$

If the exponent µ is purely real, the motion is bound,
if µ has some imaginary part x is exponantially growing and the motion is unstable.

The parameters *a* and *q* determine if the motion is stable or not.
Find solution analytically (complicated) or numerically:

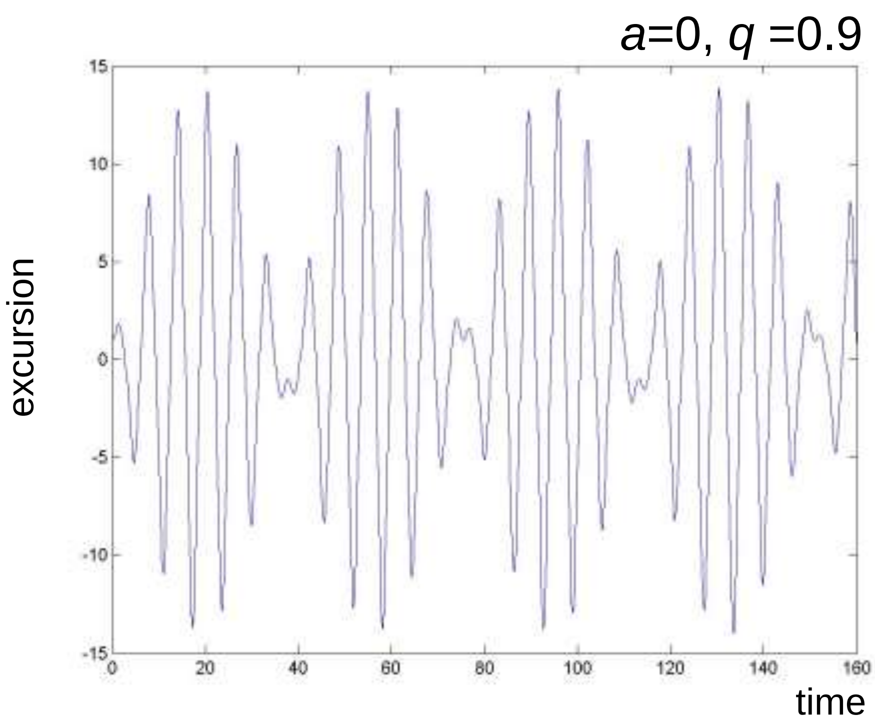

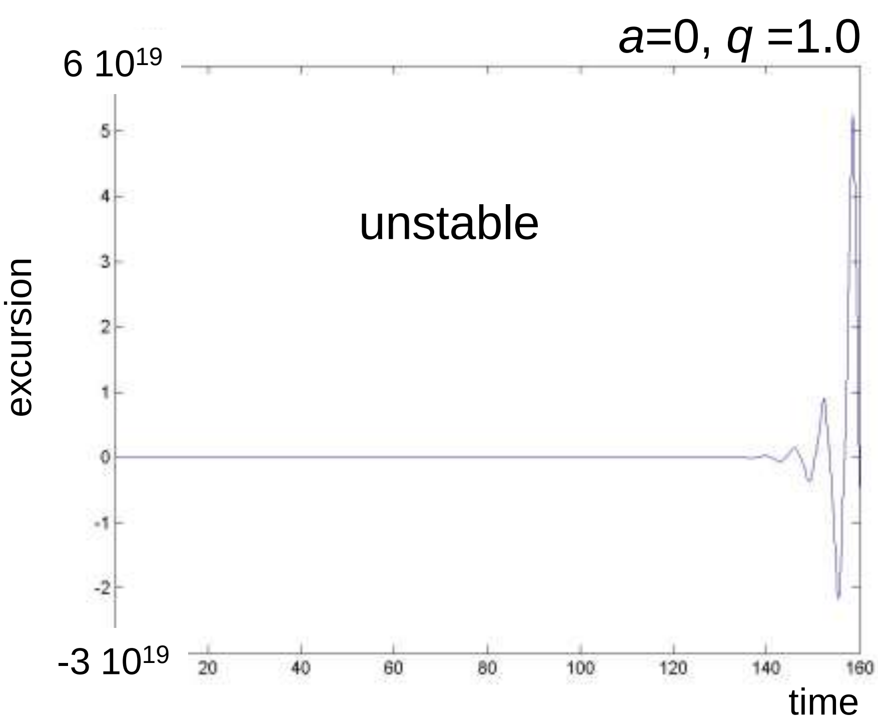

3-Dim. Paul trap stability diagram

for a << q << 1 exist approximate solutions

$$r_i(t) = r_1^0 cos(\omega_1 t + \phi_i)(1 + \tfrac{q_i}{2} cos(\Omega_{RF} t))$$

$$\boxed{\omega_i = \beta_i \frac{\Omega_{RF}}{2} \qquad \beta_i = \sqrt{a_i + \frac{q_i}{2}}}$$

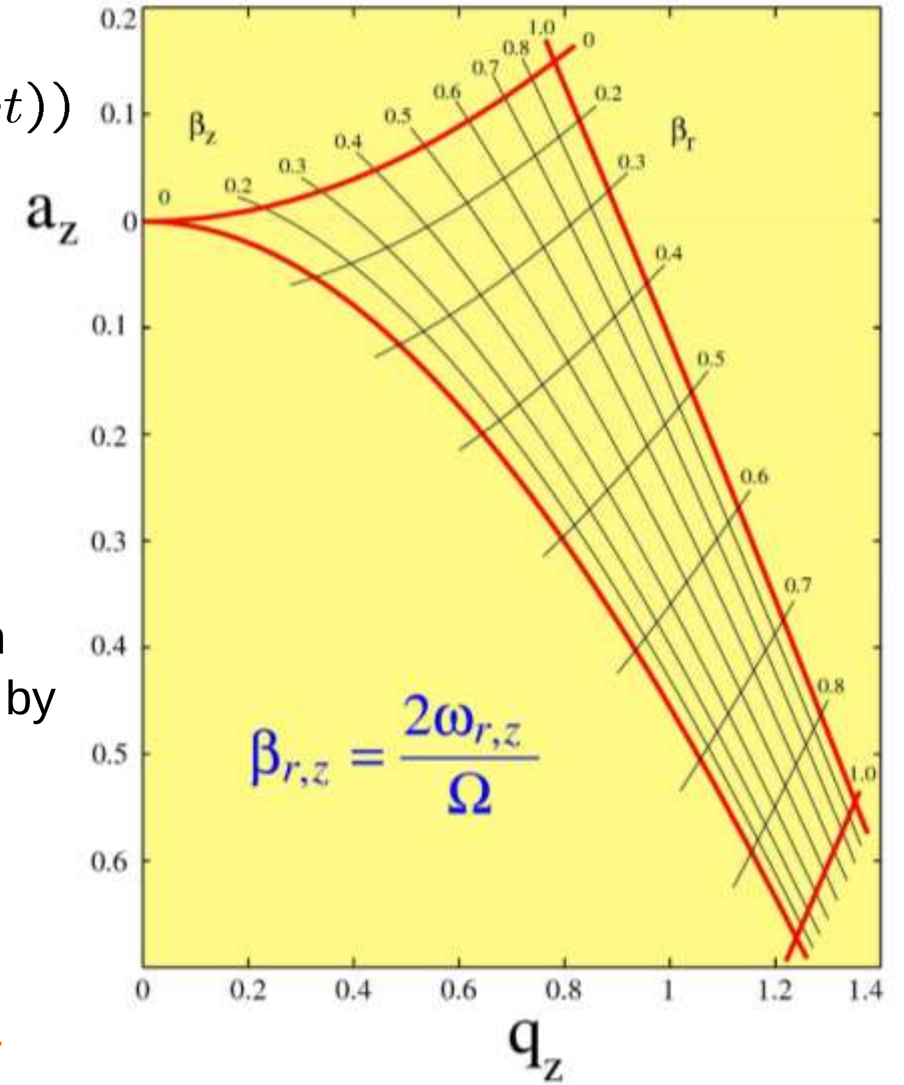

The 3D harmonic motion with frequency ω_i can be interpreted, approximated, as being caused by a pseudo-potential Ψ

$$\boxed{Q\Psi = \frac{1}{2} \sum m \omega_i^2 r_i^2, \quad i = x, y, z}$$

→ leads to a quantized harmonic oscillator

Pseudo potential approximation:
RMP 75, 281 (2003), NJP 14, 093023 (2012), PRL 109, 263003 (2012)

Real 3-Dim. Paul traps

non-ideal surfaces

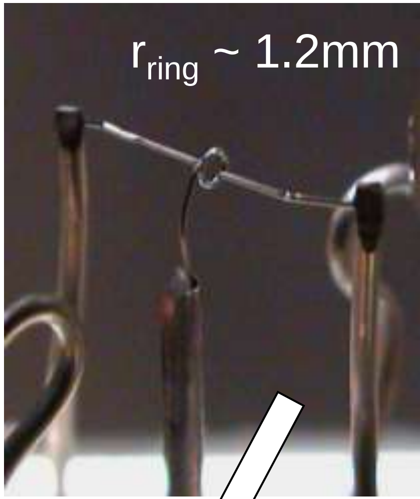

ideal 3 dim. Paul trap with equi-potential surfaces formed by copper electrodes

Fig. 6 quadrupole trap from Mainz

RMP 82, 2609 (2010)

numerical calculation of equipotential lines

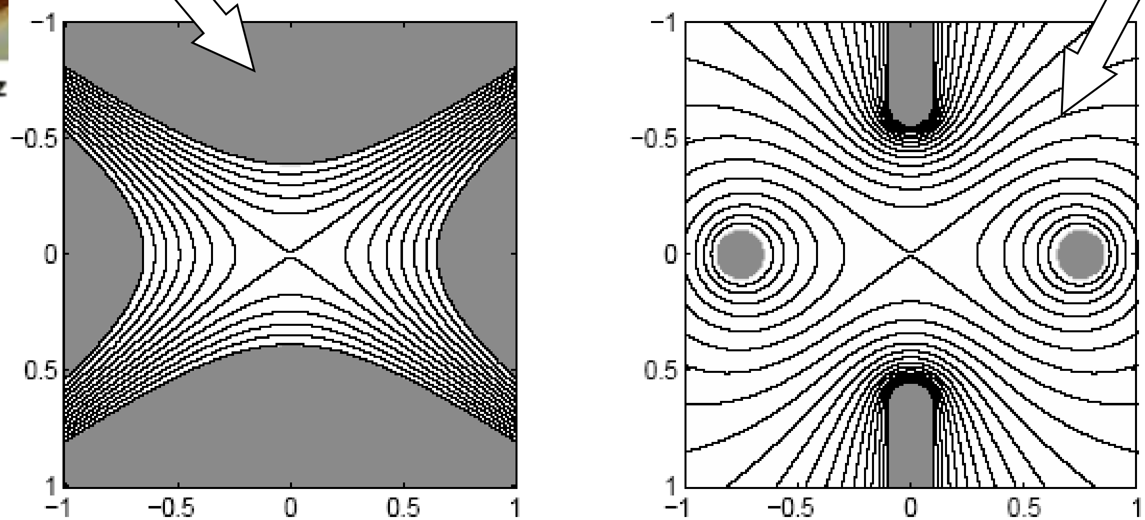

similar potential near the center

Equipotential lines of a quadrupole potential (left plot) and an approximate quadrupole potential (right). Both potentials have a cylindrical symmetry. The horizontal axis corresponds to the radial direction, the vertical axis is the symmetry axis. The electrode structure shown in the right plot is the one used for the experiments if length is measured in millimeters. It is composed of a ring electrode and two cylindrical electrodes with hemispheric endcaps.

2-Dim. Paul mass filter stability diagram

time depending potential $\Phi(x,y,t) = \Phi_0(t) \cdot (x^2 - y^2)$

with $\Phi_0(t) = (U + V cos(\Omega_{RF} t))/r_0^2$

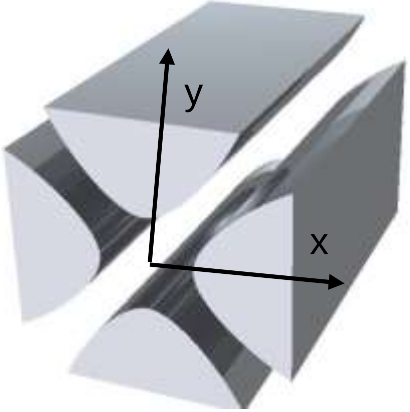

dynamical confinement in the x- y-plane

$$\boxed{\begin{aligned} \ddot{x} + (a - 2\ q\ cos(2\tau))x &= 0 \\ \ddot{y} - (a - 2\ q\ cos(2\tau))y &= 0 \end{aligned}}$$

with substitutions

$$a_i = -\frac{4QU}{mr_0^2\Omega_{RF}^2} \qquad q_i = -\frac{2QV}{mr_0^2\Omega_{RF}^2} \qquad \tau = \frac{1}{2}\Omega_{RF} t$$

radial trap radius r_0

Innsbruck design of linear ion trap

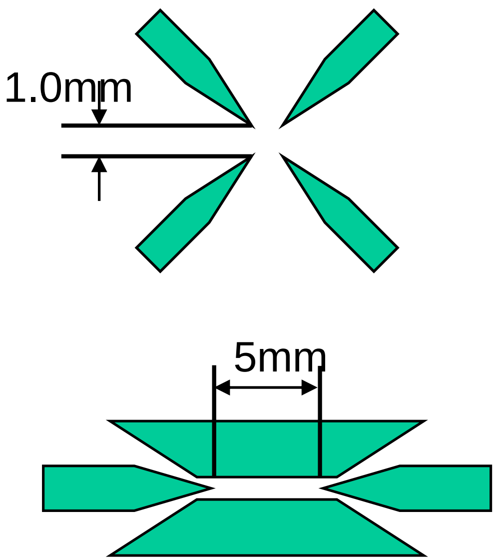

Blade design

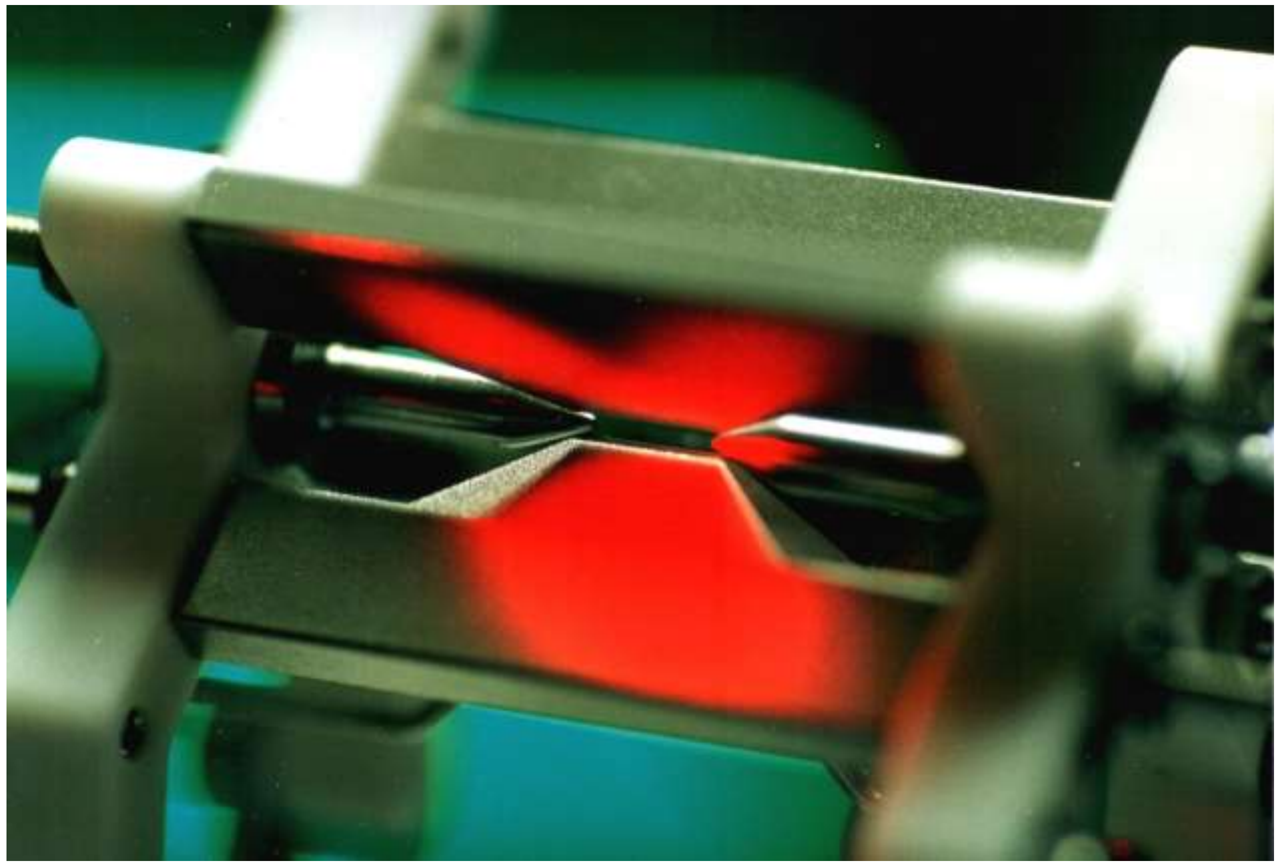

$$\omega_{axial} \approx 0.7 - 2 \text{ MHz} \qquad \omega_{radial} \approx 5 \text{ MHz}$$

$$trap\ depth \approx eV$$

F. Schmidt-Kaler, et al., Appl. Phys. B 77, 789 (2003).

Ion crystals:
Equilibrium positions and eigenmodes

Equilibrium positions in the axial potential

$$V = \sum_{m=1}^{N} \frac{1}{2} M\nu^2 x_m(t)^2 + \sum_{\substack{n,m=1\\ m\neq n}}^{N} \frac{Z^2e^2}{8\pi\epsilon_0}\frac{1}{|x_n(t)-x_m(t)|},$$

trap potential   mutual ion repulsion

z-axis

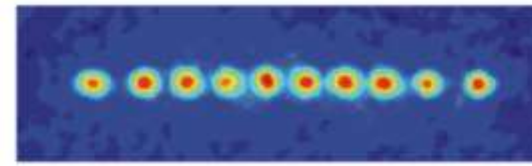

find equilibrium positions x^0: $x_m(t) \approx x_m^{(0)} + q_m(t)$ ions oscillate with *q(t)* arround

condition for equilibrium: $(\partial V/\partial x_m)_{x_m = x_m^{(0)}} = 0$

dimensionless positions $u_m = x_m^{(0)}/l$ with length scale $l^3 = \frac{Z^2e^2}{4\pi\epsilon_0 M\omega_{ax}^2}$

$^{40}Ca^{+} at\ 1MHz \rightarrow 4.5\mu m$

$$\longrightarrow \quad u_m - \sum_{n=1}^{m-1}\frac{1}{(u_m-u_n)^2} + \sum_{n=m+1}^{N}\frac{1}{(u_m-u_n)^2} = 0$$

$$(m = 1, 2, \ldots N).$$

D. James, Appl. Phys. B 66, 181 (1998)

Equilibrium positions in the axial potential

$$u_m - \sum_{n=1}^{m-1} \frac{1}{(u_m - u_n)^2} + \sum_{n=m+1}^{N} \frac{1}{(u_m - u_n)^2} = 0$$

$$(m = 1, 2, \ldots N)\,.$$

set of N equations for u_m

force of the trap potential

Coulomb force of all ions from left side

Coulomb force of all ions from left side

numerical solution (Mathematica), e.g. *N=5* ions

```
(* N=5 *)
Clear[a, a1, a2, a3, a4, a5, a6, a7, a8, a9, a10]
 lösche
a = Table[{a1, a2, a3, a4, a5, a6, a7, a8, a9, a10}, ];
 Tabelle
equ5 = Table[a[[m]]
 Tabelle
  - Sum[1 / (a[[m]] - a[[n]])^2, {n, 1, m - 1}]
   summiere
  + Sum[1 / (a[[m]] - a[[n]])^2, {n, m + 1, 5}], {m, 1, 5}]
   summiere
aa5 = Timing[FindRoot[equ5, {a1, -10}, {a2, -1}, {a3, 0.1}, {a4, 1}, {a5, 10}]]
 Dauer   ermittle Nullstelle
```

$$\left\{a1 + \frac{1}{(a1-a2)^2} + \frac{1}{(a1-a3)^2} + \frac{1}{(a1-a4)^2} + \frac{1}{(a1-a5)^2},\ a2 - \frac{1}{(-a1+a2)^2} + \frac{1}{(a2-a3)^2} + \frac{1}{(a2-a4)^2} + \frac{1}{(a2-a5)^2},\ a3 - \frac{1}{(-a1+a3)^2} - \frac{1}{(-a2+a3)^2} + \frac{1}{(a3-a4)^2} + \frac{1}{(a3-a5)^2},\right.$$
$$\left. a4 - \frac{1}{(-a1+a4)^2} - \frac{1}{(-a2+a4)^2} - \frac{1}{(-a3+a4)^2} + \frac{1}{(a4-a5)^2},\ a5 - \frac{1}{(-a1+a5)^2} - \frac{1}{(-a2+a5)^2} - \frac{1}{(-a3+a5)^2} - \frac{1}{(-a4+a5)^2}\right\}$$

$\{0.01\ \text{Second}, \{a1 \to -1.7429, a2 \to -0.822101, a3 \to 1.2717 \times 10^{-17}, a4 \to 0.822101, a5 \to 1.7429\}\}$

```
aa5[[2]][[2]][[2]]
-0.822101
abs5 = Table[aa5[[2]][[i]][[2]], {i, 1, 5}]
 Tabelle
```

$\{-1.7429, -0.822101, 1.2717 \times 10^{-17}, 0.822101, 1.7429\}$

equilibrium positions $\boxed{-1.74 \quad -0.82 \quad 0 \quad +0.82 \quad +1.74}$

Eigenmodes and Eigenfrequencies

Lagrangian of the axial ion motion: $L = T + V$

describes small excursions arround equilibrium positions

$$= \frac{M}{2}\sum_{m=1}^{N}(\dot{q}_m)^2 - \frac{1}{2}\sum_{m,n=1}^{N} q_n q_n \left(\frac{\partial^2 V}{\partial x_n \partial x_m}\right)_0 + \ldots$$

$$= \frac{M}{2}\left(\sum_{m=1}^{N} \dot{q}_m^2 - \omega_{ax}^2 \sum_{m,n=1}^{N} A_{nm} q_n q_n\right)$$

D. James, Appl. Phys. B 66, 181 (1998)

with $$A_{mn} = 1 + 2\sum_{\substack{n \neq m \\ n = 0}}^{N} \frac{1}{|u_m - u_n|^3} \quad if \quad m = n$$

and $$A_{mn} = -\frac{2}{|u_m - u_n|^3} \quad if \quad m \neq n$$

linearized Coulomb interaction leads to Eigenmodes, but the next term in Tailor expansion leads to mode coupling, which is however typically very small.

C. Marquet, et al., Appl. Phys. B 76, 199 (2003)

Eigenmodes and Eigenfrequencies

numerical solution (Mathematica), e.g. *N=4* ions

```
(*      N=4      AXIAL         *************************)
A4 = Table[
      Tabelle
    If[m != n,
    wenn
     -2 / Abs[u4[[m]] - u4[[n]]]^3,
          Absolutwert
     1. + 2 Sum[ If[ i ≠ m, 1. / Abs[(u4[[m]] - u4[[i]])^3] , 0], {i, 1, 4}]  ],
            s···  wenn          Absolutwert
                                  {m, 1, 4}, {n, 1, 4}];
```

Matrix, to diagonize

```
TableForm[Eigenvectors[A4]]
Tabellendar··  Eigenvektoren
freq4 = Sqrt[Eigenvalues[A4]]   (* Modenfrequenzen *)
        Qua··  Eigenwerte
TableForm[A4];
Tabellendarstellung
```

-0.213213	0.674196	-0.674196	0.213213
0.5	-0.5	-0.5	0.5
-0.674196	-0.213213	0.213213	0.674196
-0.5	-0.5	-0.5	-0.5

{3.05096, 2.41039, 1.73205, 1.}

Eigenvectors pictorial

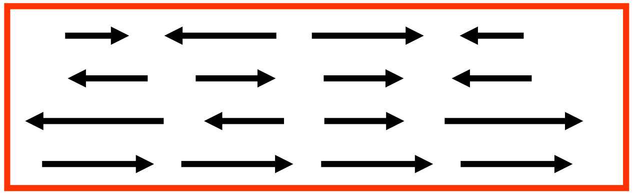

Eigenvalues

$$(3.059 \pm 0.008)\omega_{ax} \quad \sqrt{29/5}\omega_{ax} \quad \sqrt{3}\omega_{ax} \quad 1\omega_{ax}$$

depends on *N* does not

for the radial modes: *Market et al., Appl. Phys. B76, (2003) 199*

Common mode excitations

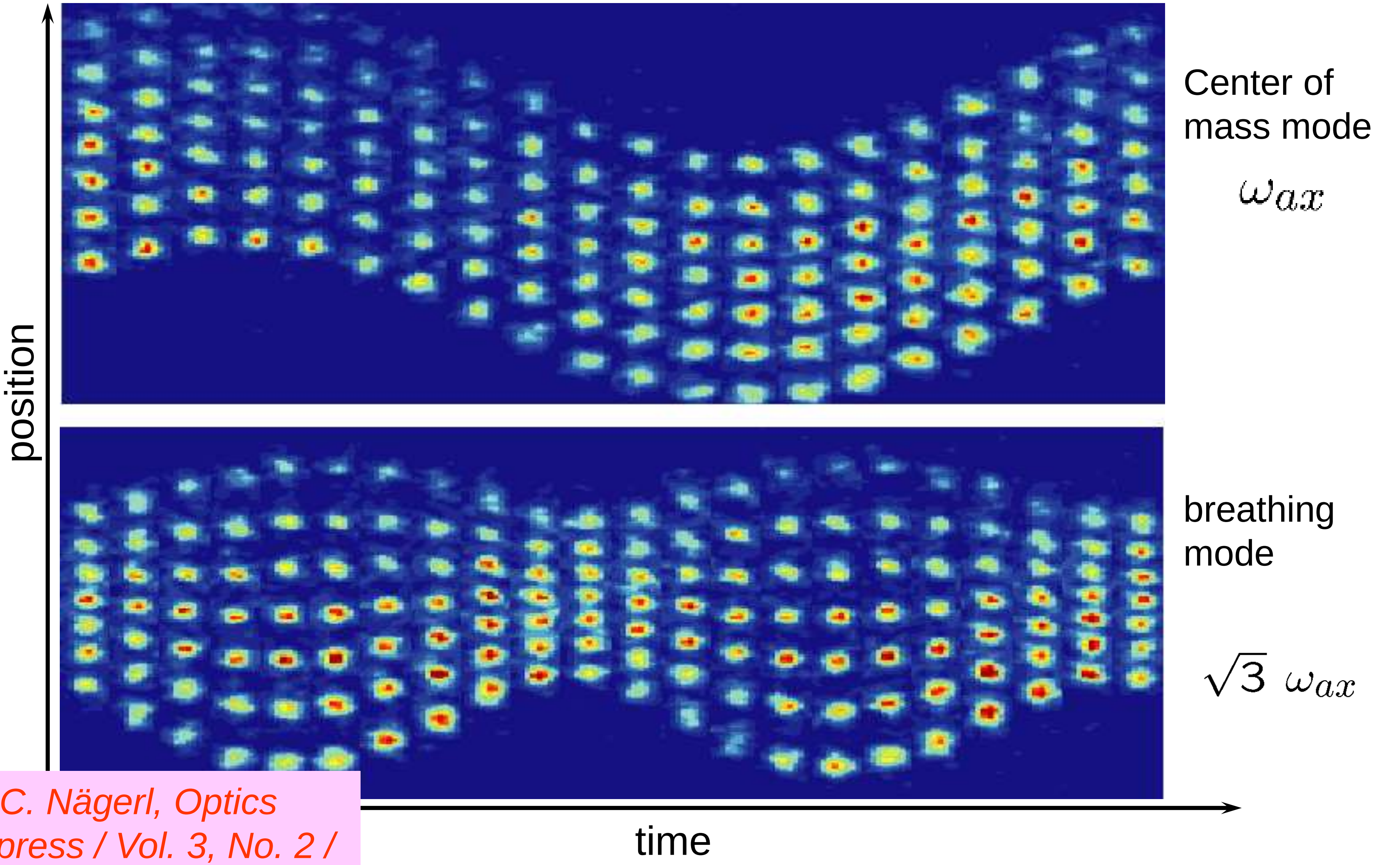

H. C. Nägerl, Optics Express / Vol. 3, No. 2 / 89 (1998).

Breathing mode excitation

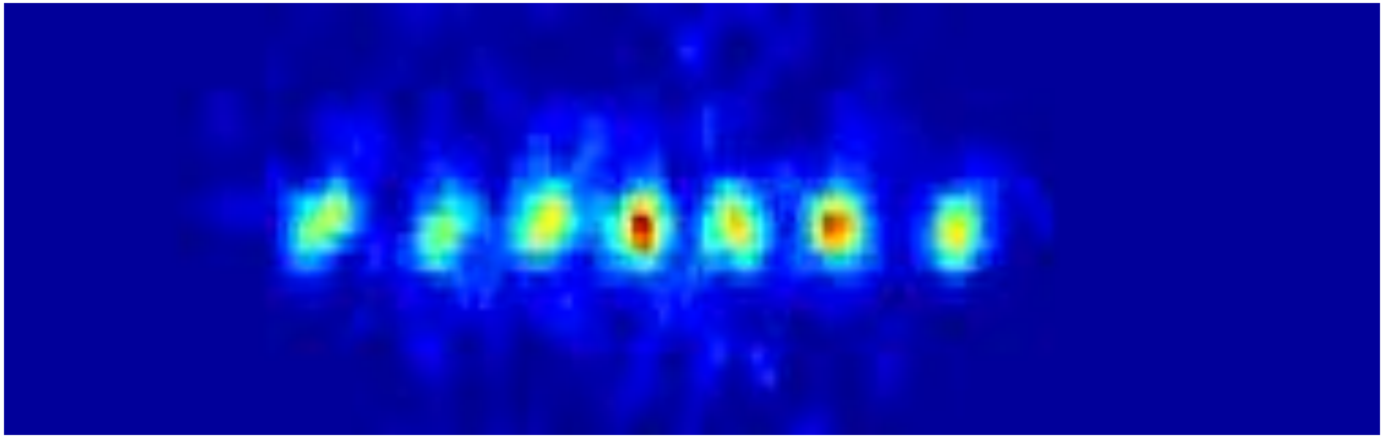

H. C. Nägerl, Optics Express / Vol. 3, No. 2 / 89 (1998).

1D, 2D, 3D ion crystals

Wineland et al., J. Res. Natl. Inst. Stand. Technol. 103, 259 (1998)

- Depends on $\alpha=(\omega_{ax}/\omega_{rad})^2$
- Depends on the number of ions $a_{crit}= cN^{\beta}$

Enzer et al., PRL85, 2466 (2000)

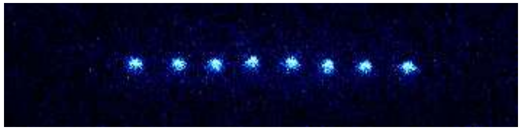

1D

- Generate a planar Zig-Zag when $\omega_{ax} < \omega^{y}_{rad} << \omega^{x}_{rad}$
- Tune radial frequencies in y and x direction

Planar crystal equilibrium positions

2D

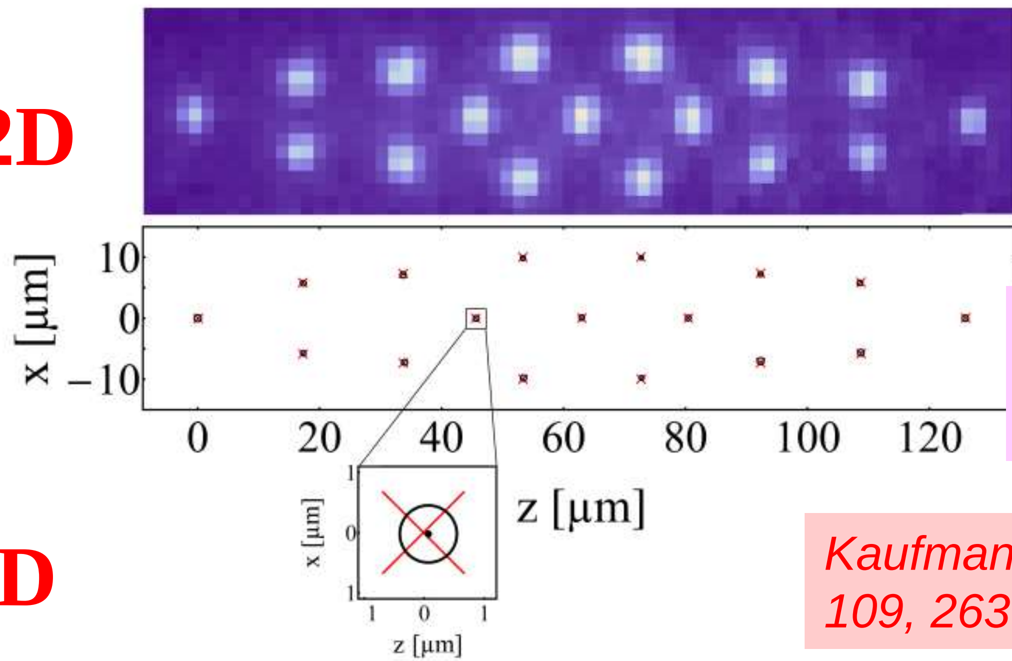

δx~50nm ±0.25%

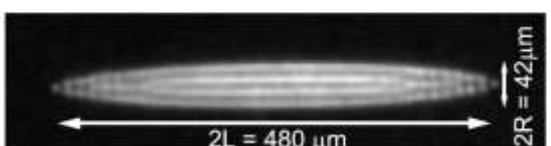

3D

Kaufmann et al, PRL 109, 263003 (2012)

Ion crystal beyond harmonic approximations

$$H = \sum_{i,\mu} \left(\frac{p_{i\mu}^2}{2m} + \frac{1}{2} m \omega_\mu^2 r_{i\mu}^2 \right) + \frac{1}{2} \sum_{i \neq j} \frac{e^2}{4\pi\varepsilon_0} \frac{1}{|\mathbf{r}_i - \mathbf{r}_j|}$$

E_{kin} $U_{pot,harm.}$ $U_{Coulomb}$

Marquet, Schmidt-Kaler, James, Appl. Phys. B 76, 199 (2003)

$$H^{(3)} = 3 \frac{z_0}{4l_z} \hbar\omega_z \sum_{n,m,p} \frac{D_{nmp}^{(3)}}{\sqrt[4]{\gamma_n^x \gamma_m^x \lambda_p^z}} (a_n + a_n^\dagger)(a_m + a_m^\dagger)(c_p + c_p^\dagger)$$

$$H^{(4)} = 3 \left(\frac{z_0}{4l_z} \right)^2 \hbar\omega_z \sum_{n,m,p,q} D_{nmpq}^{(4)} \frac{(a_n + a_n^\dagger)(a_m + a_m^\dagger)}{\sqrt[4]{\gamma_n^x \gamma_m^x}} \left[\frac{(a_p + a_p^\dagger)(a_q + a_q^\dagger)}{\sqrt[4]{\gamma_p^x \gamma_q^x}} + \frac{2(b_p + b_p^\dagger)(b_q + b_q^\dagger)}{\sqrt[4]{\gamma_p^y \gamma_q^y}} - \frac{8(c_p + c_p^\dagger)(c_q + c_q^\dagger)}{\sqrt[4]{\lambda_p^z \lambda_q^z}} \right].$$

Z_0 wavepaket size

l_z ion distance

γ,λ ion frequencies

$D_{n,m,p}$ coupling matrix

Non-linear couplings in ion crystal

$$H_{\mathrm{eff}}^{(4)} = H_{\mathrm{s}} + H_{\mathrm{d}}$$

$$H_{\mathrm{s}} = \hbar \frac{\Omega_{\mathrm{SI}}}{2} (a_{\mathrm{zz}}^{\dagger})^2 a_{\mathrm{zz}}^2 + \hbar \Delta\omega_{\mathrm{zz}} a_{\mathrm{zz}}^{\dagger} a_{\mathrm{zz}}$$

Self-interaction

$$H_{\mathrm{d}} = a_{\mathrm{zz}}^{\dagger} a_{\mathrm{zz}} \left(\hbar \Omega_{\mathrm{d},2}^{x} a_2^{\dagger} a_2 + \hbar \sum_{n=2,3} \Omega_{\mathrm{d,n}}^{y} b_n^{\dagger} b_n + \Omega_{\mathrm{d,n}}^{z} c_n^{\dagger} c_n \right)$$

Cross
Kerr coupling

$$H_{\mathrm{res}}^{(3)} = \hbar \Omega_{\mathrm{T}} [a_{\mathrm{zz}}^2 c_{\mathrm{str}}^{\dagger} + (a_{\mathrm{zz}}^{\dagger})^2 c_{\mathrm{str}}]$$

Resonant inter-mode coupling

…. remind yourself of non-linear optics: frequency doubling, Kerr effect, self-phase modulation, ….

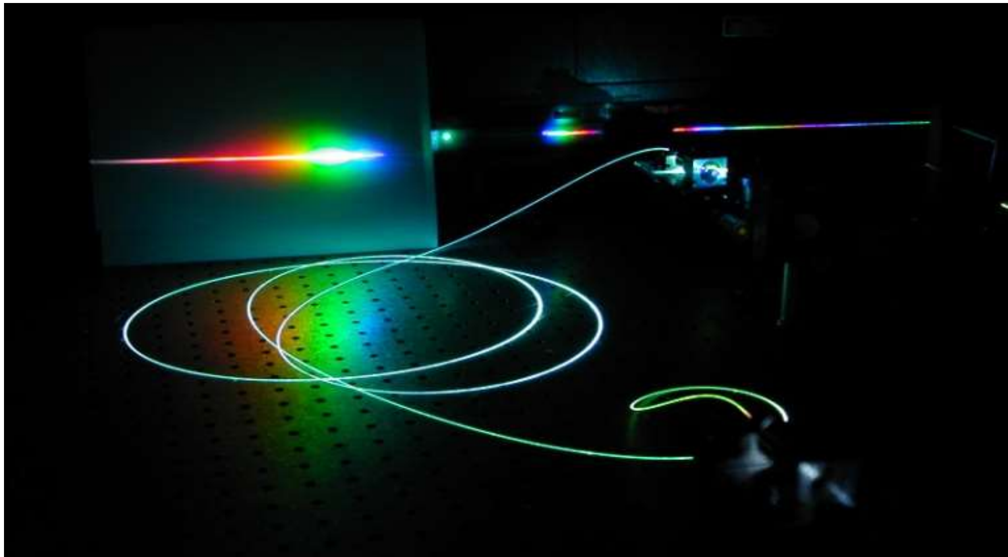

Lemmer, Cormick, Schmiegelow, Schmidt-Kaler, Plenio, PRL 114, 073001 (2015)

Non-linear couplings in ion crystal

Ding, et al, PRL119, 193602 (2017)

Cross
Kerr coupling

$$H_{\mathrm{d}} = a_{\mathrm{zz}}^{\dagger} a_{\mathrm{zz}} \left(\hbar \Omega_{\mathrm{d},2}^{x} a_{2}^{\dagger} a_{2} + \hbar \sum_{n=2,3} \Omega_{\mathrm{d,n}}^{y} b_{n}^{\dagger} b_{n} + \Omega_{\mathrm{d,n}}^{z} c_{n}^{\dagger} c_{n} \right)$$

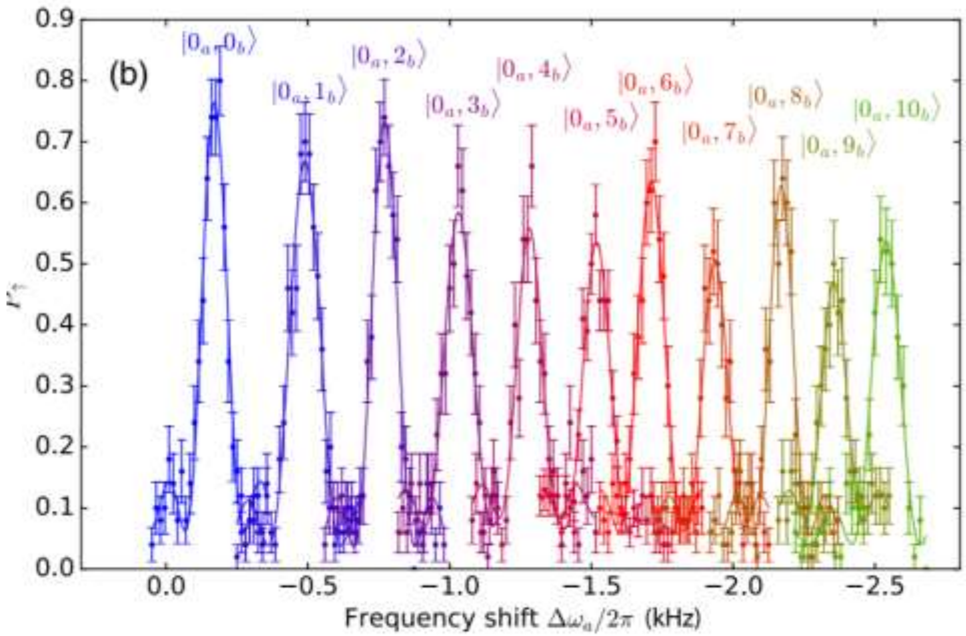

Frequ. of mode a depends on occupation in mode b

two phonons in mode b generate one phonon in mode a

Resonant inter-mode coupling

$$H_{\mathrm{res}}^{(3)} = \hbar \Omega_{\mathrm{T}} [a_{\mathrm{zz}}^{2} c_{\mathrm{str}}^{\dagger} + (a_{\mathrm{zz}}^{\dagger})^{2} c_{\mathrm{str}}]$$

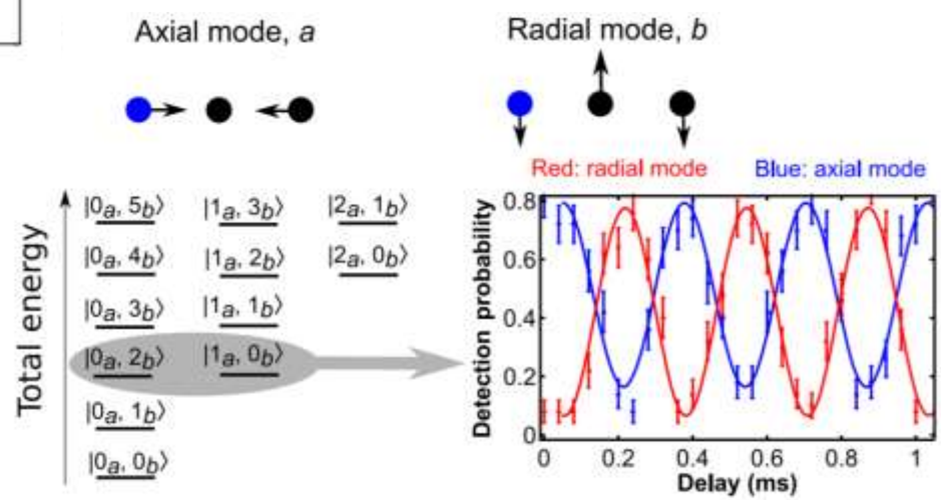

Basics: Harmonic oscillator

Why? The trap confinement is leads to three independend harmonic oscillators !

$$E = E_{kin} + E_{pot} = \frac{\vec{p}^2}{2m} + \frac{m}{2}\omega_{ax}^2 x^2$$

here only for the linear direction of the linear trap ⟶ no micro-motion

treat the oscillator quantum mechanically and introduce *a*+ and *a*

$$x = \sqrt{\frac{\hbar}{2m\omega_{ax}}}(a + a^\dagger) \qquad p_x = i\sqrt{\frac{\hbar m\omega_{ax}}{2}}(a^\dagger - a)$$

and get Hamiltonian

$$\boxed{H_{oscillator} = \hbar\omega_{ax}(a^\dagger a + \frac{1}{2})}$$

Eigenstates |*n*> with:

$$H|n\rangle = \hbar\omega_{ax}(n + \frac{1}{2})|n\rangle$$

$$a^\dagger|n\rangle = \sqrt{n}|n-1\rangle$$

$$a|n\rangle = \sqrt{n+1}|n+1\rangle$$

Harmonic oscillator wavefunctions

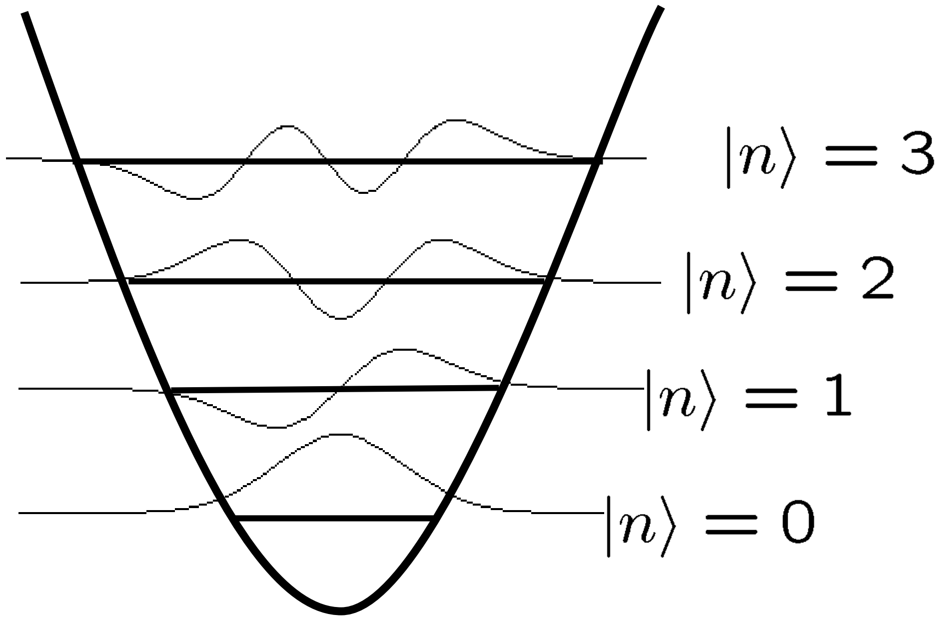

Eigen functions

$$u(x) \sim H(n,x)\; e^{-x^2}$$

with orthonormal Hermite polynoms
and energies:

$$E(n) = \hbar\omega_{ax}(n + \tfrac{1}{2})$$

Two – level atom

Why? Is an idealization which is a good approximation to real physical system in many cases

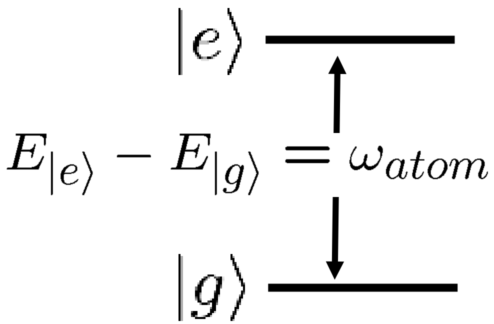

$$\boxed{\begin{aligned} H_{atom} &= \hbar\omega_{atom}(|e\rangle\langle e| - |g\rangle\langle g|) \\ &= \hbar\omega_{atom}\sigma_z \end{aligned}}$$

two level system is connected with spin ½ algebra using the Pauli matrices

$$\boxed{\begin{aligned} |g\rangle\langle g| + |e\rangle\langle e| &\rightarrow \hat{I} \\ |g\rangle\langle e| + |e\rangle\langle g| &\rightarrow \hat{\sigma_x} \\ i(|g\rangle\langle e| - |e\rangle\langle g|) &\rightarrow \hat{\sigma_y} \\ |e\rangle\langle e| - |g\rangle\langle g| &\rightarrow \hat{\sigma_z} \end{aligned}}$$

D. Leibfried, C. Monroe,
R. Blatt, D. Wineland,
Rev. Mod. Phys. 75, 281 (2003)

Two – level atom

Why? Is an idealization which is a good approximation to real pyhsical system in many cases

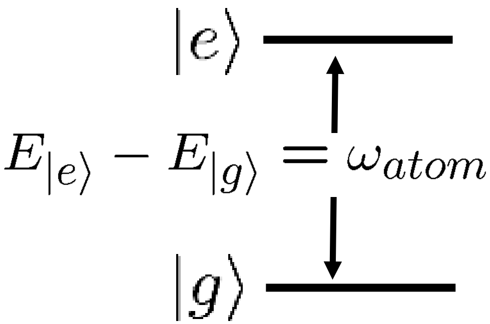

$$\boxed{\begin{aligned} H_{atom} &= \hbar\omega_{atom}(|e\rangle\langle e| - |g\rangle\langle g|) \\ &= \hbar\omega_{atom}\sigma_z \end{aligned}}$$

together with the harmonic oscillator leading to the ladder of eigenstates |g,n>, |e,n>:

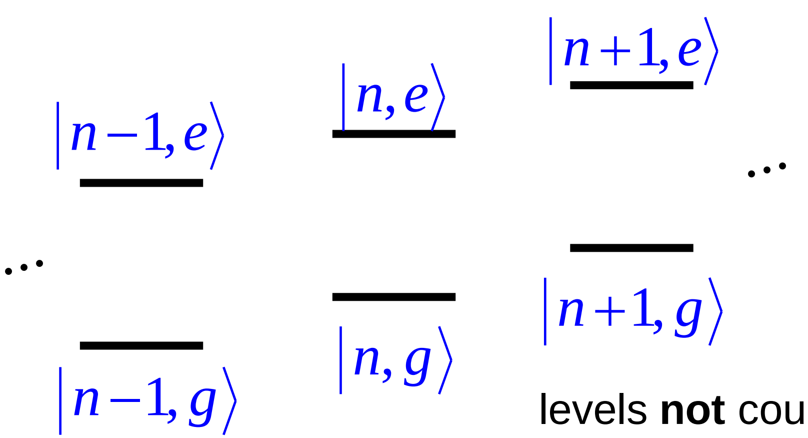

$$\boxed{H_0 = \frac{p^2}{2m_0} + \frac{1}{2}m_0\omega^2x^2 + \frac{1}{2}\hbar\omega_a\sigma_z}$$

levels **not** coupled

Laser coupling

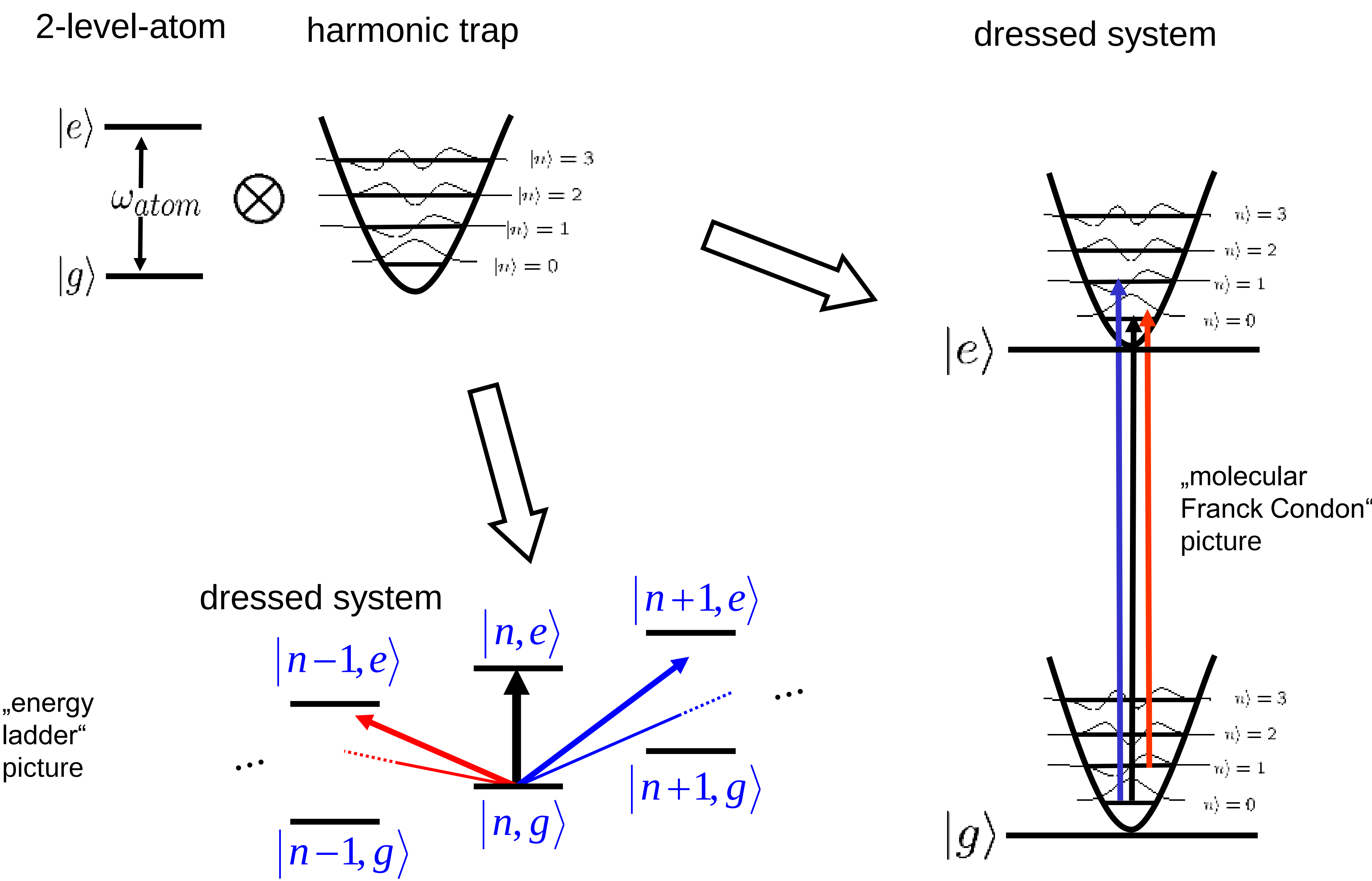

Laser coupling

dipole interaction, Laser radiation with frequency ω_l, and intensity $|E|^2$

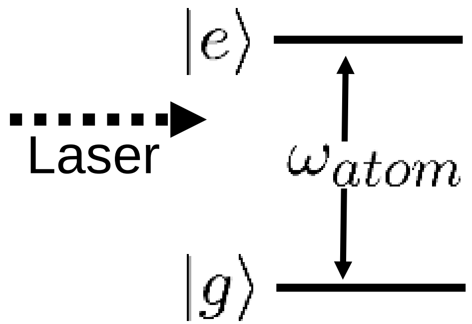

Rabi frequency: $\Omega_R = \langle g|\vec{d}\cdot\vec{E}|e\rangle$

$$\boxed{\begin{aligned} H_{ge} &= \hbar\frac{\Omega_R}{2}(|g\rangle\langle e| + |e\rangle\langle g|) \\ &= \hbar\frac{\Omega_R}{2}(\sigma^+ + \sigma^-) \end{aligned}}$$

with
$$\begin{aligned} |e\rangle\langle g| &\rightarrow \sigma^+ = (\sigma_x + i\sigma_y)/2 \\ |g\rangle\langle e| &\rightarrow \sigma^- = (\sigma_x - i\sigma_y)/2 \end{aligned}$$

the laser interaction (running laser wave) has a spatial dependence:

$$\vec{d}\cdot\vec{E} \longrightarrow \vec{d}\cdot\vec{E}e^{ikx}$$

momentum kick, recoil: e^{ikx}

$$\boxed{\begin{aligned} H_{ge} &= \hbar\frac{\Omega_R}{2}(|g\rangle\langle e|e^{ikx} + |e\rangle\langle g|e^{-ikx}) \\ &= \tfrac{1}{2}\hbar\Omega(\sigma^+ + \sigma^-)(e^{i(kx-\omega_l t+\phi)} + e^{-i(kx-\omega_l t+\phi)}) \end{aligned}}$$

Laser coupling

in the rotating wave approximation

$$\boxed{H_{ge} = \frac{1}{2}\hbar\Omega(\sigma^+ e^{i(\eta(a+a^\dagger)} e^{-i\omega_l t} + \sigma^- e^{-i\eta(a+a^\dagger)} e^{\omega_l t})}$$

using $x = \sqrt{\frac{\hbar}{2m\omega_{ax}}}(a + a^\dagger)$

and defining the Lamb Dicke parameter η:

$$\boxed{\eta = k\sqrt{\frac{\hbar}{2m\omega_{ax}}}}$$

if the laser direction is at an angle ϕ to the vibration mode direction:

single photon transition

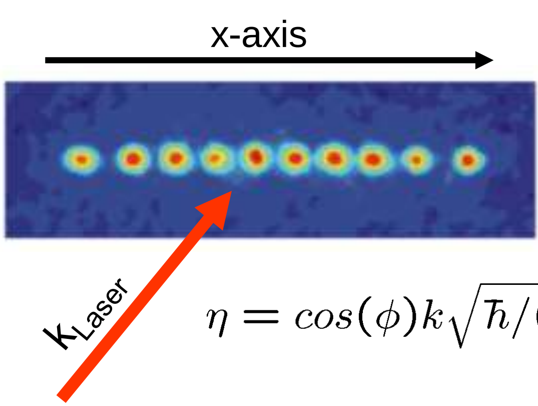

$\eta = cos(\phi)k\sqrt{\hbar/(2m\omega_{ax}}$

Raman transition: projection of $\Delta k = k_1 - k_2$

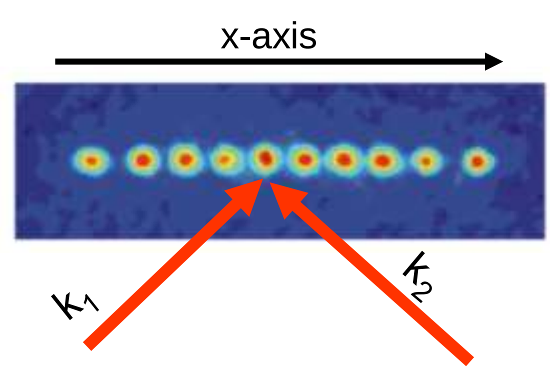

Lamb Dicke Regime

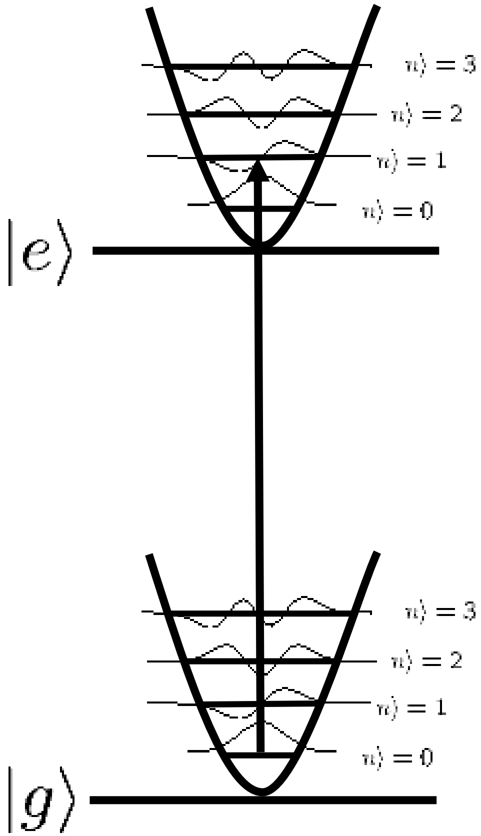

$$\langle g, n|\vec{d}\cdot\vec{E}e^{ikx}|e, m\rangle =$$

$$\langle g|\vec{d}\cdot\vec{E}|e\rangle\langle n|e^{ikx}|m\rangle =$$

$$\hbar\frac{\Omega_{Rabi}}{2}\langle n|e^{i\eta(a+a^\dagger)}|m\rangle \approx$$

$$\boxed{\eta^2(a+a^\dagger)^2 << 1 \rightarrow \eta^2(2n+1) << 1}$$

$$\hbar\frac{\Omega_{Rabi}}{2}\langle n|1+(i\eta(a+a^\dagger)|m\rangle =$$

$$\boxed{\hbar\frac{\Omega_{Rabi}}{2}\left(\delta_{n,m}+i\eta\sqrt{n}\delta_{m=n-1}+i\eta\sqrt{n+1}\delta_{m=n+1}\right)}$$

laser is tuned to the resonances:

carrier: $\Omega_{Rabi}\left(1-\eta^2(2n+1)\right)$

blue sideband: $\Omega_{Rabi}\ \eta\sqrt{n+1}$

red sideband: $\Omega_{Rabi}\ \eta\sqrt{n}$

Wavefunctions in momentum space

$$\eta = \sqrt{\frac{\hbar k}{2m\omega_{trap}}} = \sqrt{\frac{\omega_{recoil}}{\omega_{trap}}}$$

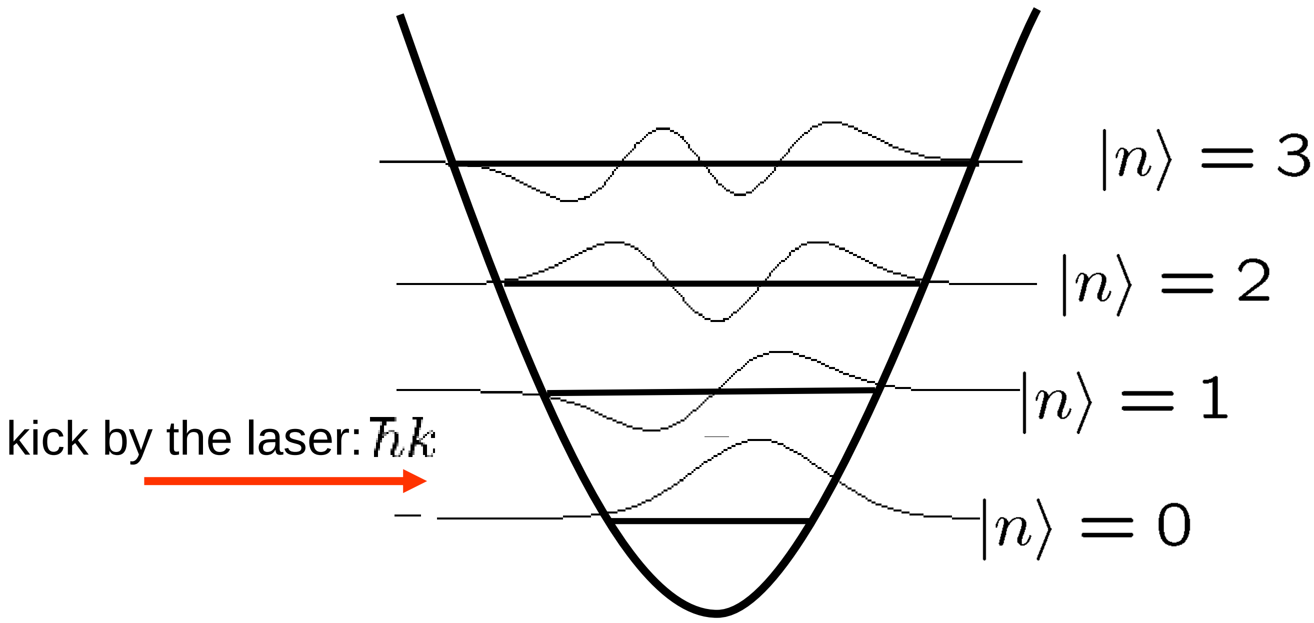

kicked wave function is **non-**orthogonal to the other wave functions

Experimental example

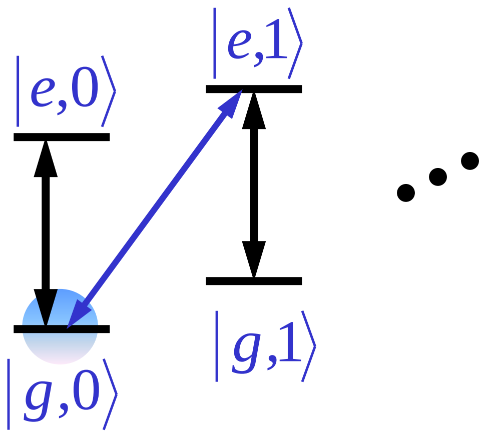

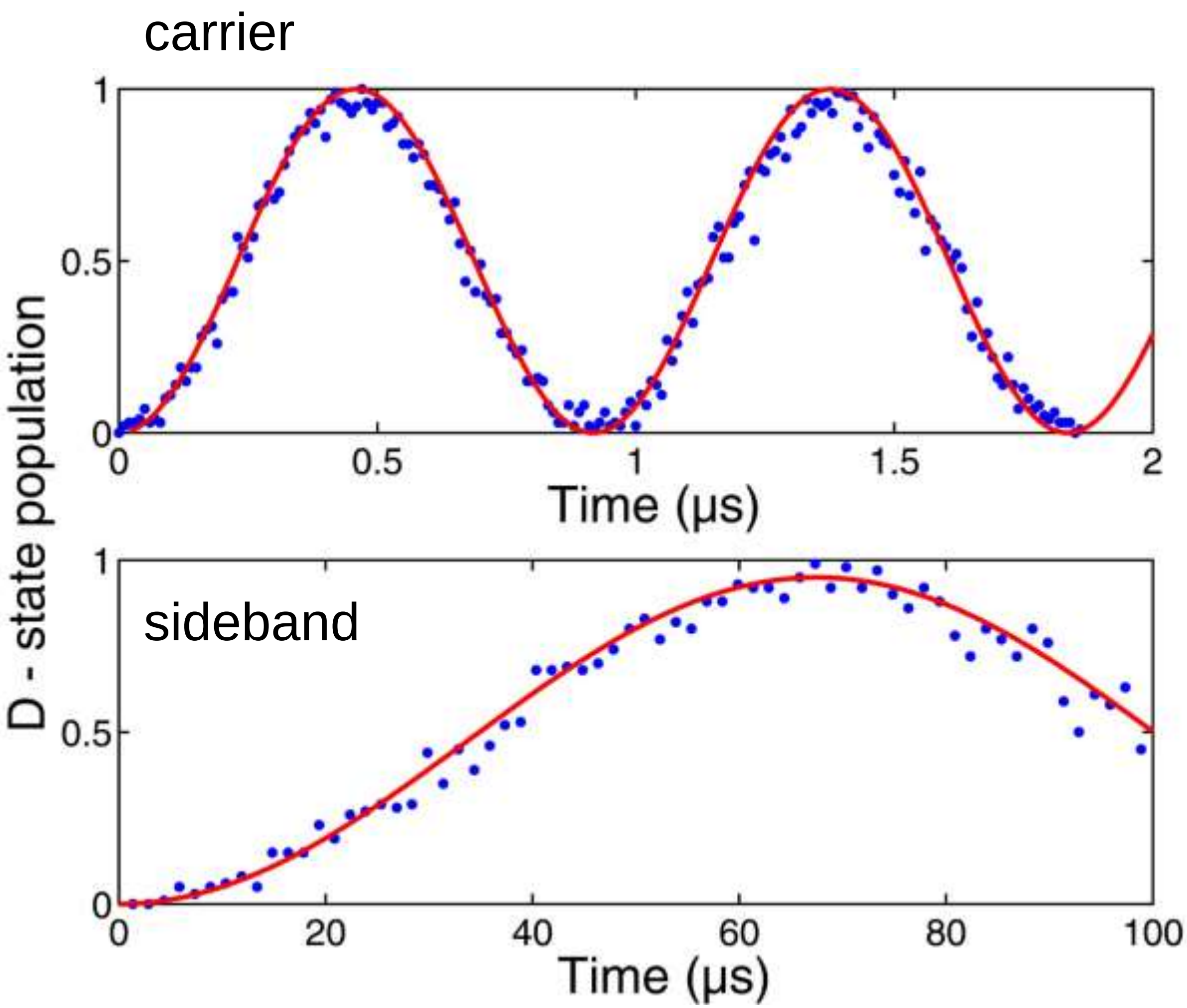

carrier and sideband
Rabi oscillations
with Rabi frequencies

Ω_{Rabi} and $\Omega_{Rabi}\ \eta$

„Weak confinement“

$$\boxed{\omega_{trap} << \gamma}$$

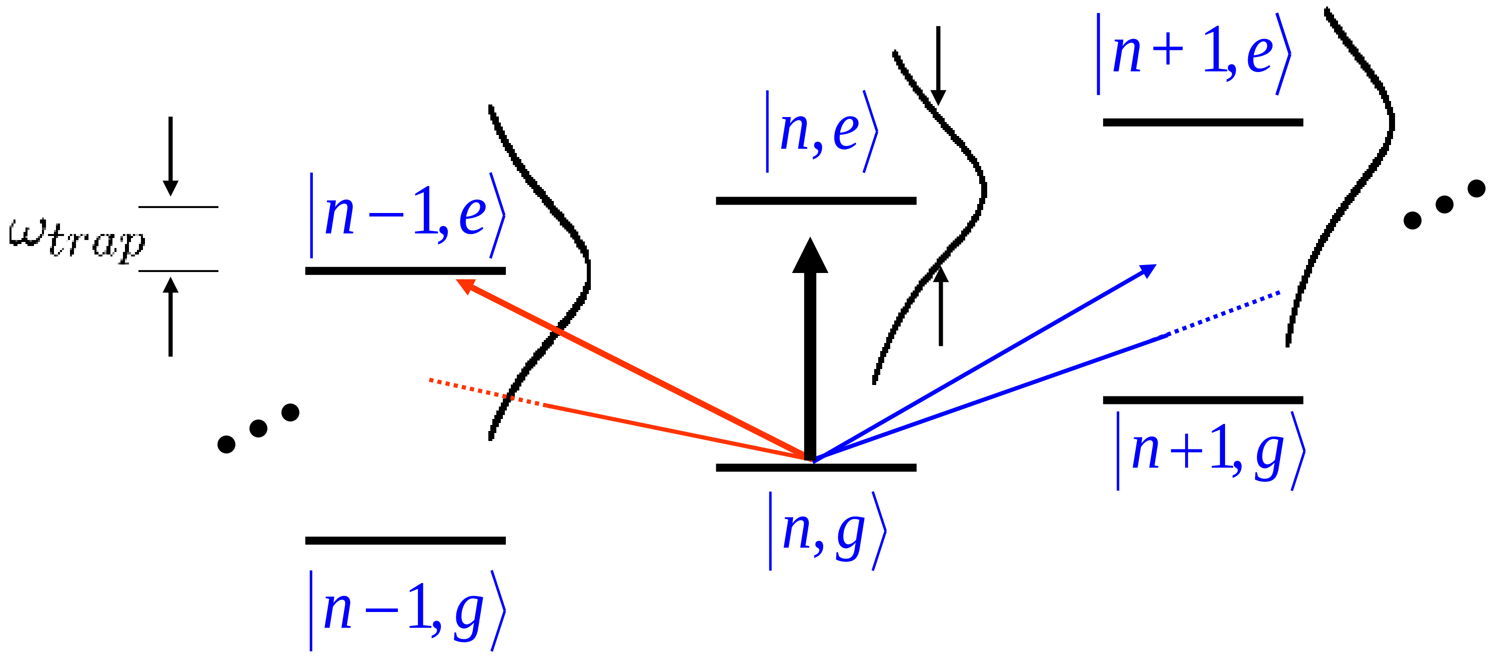

weak confinement:
Sidebands are not resolved on that transition.
Simultaneous excitation of several vibrational states

Two-level system dynamics

spont. decay rate γ

Rabi frequency Ω

incoherent: $\Omega < \gamma$

coherent: $\Omega > \gamma$

Solution of
optical Bloch equations

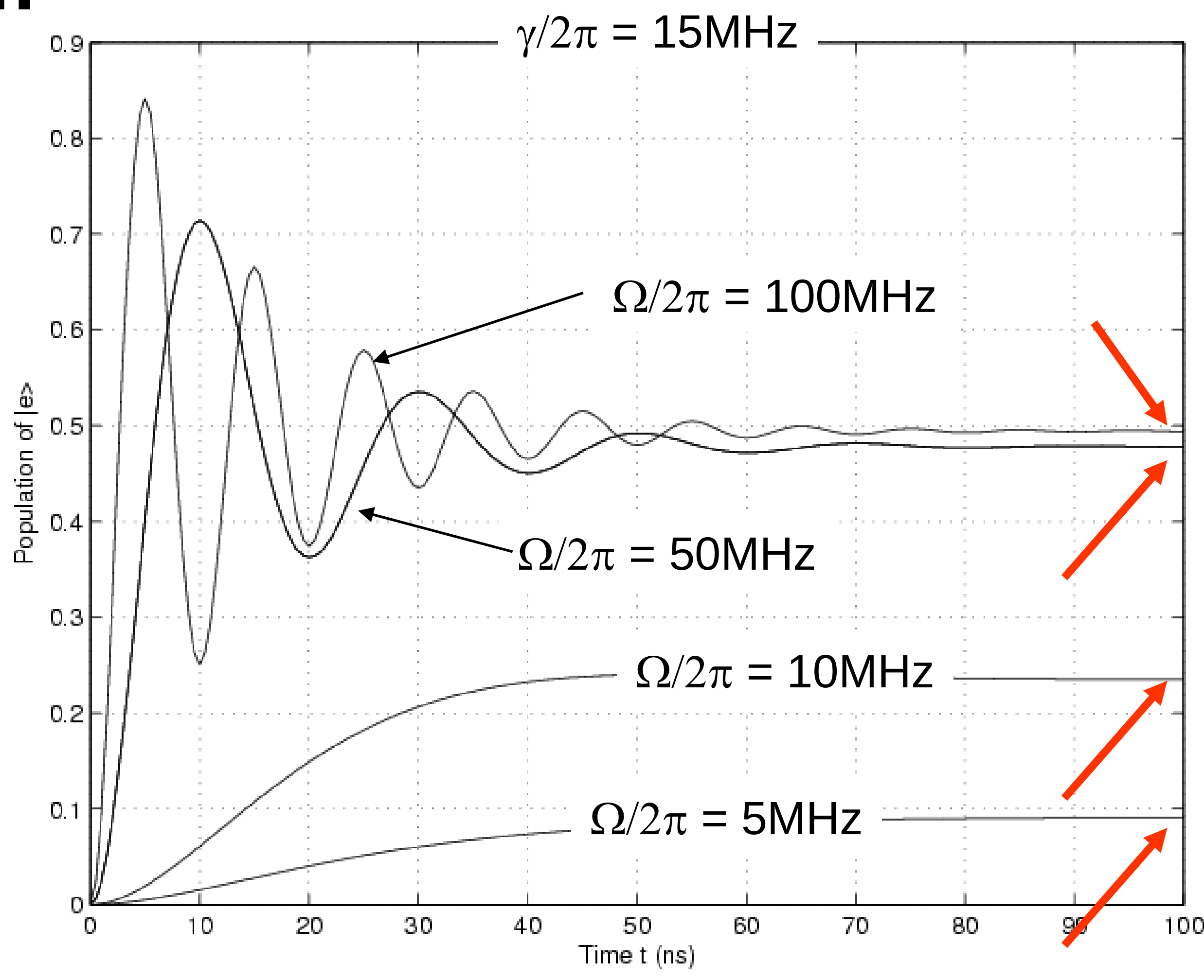

Steady state population of |e>:

$$\rho_{ee}(t \to \infty) = \frac{(\Omega/2)^2}{\Delta^2+(\gamma/2)^2+2(\Omega/2)^2} \simeq (\tfrac{\Omega}{\gamma})^2 \frac{1}{1+(2\Delta/\gamma)^2} = (\tfrac{\Omega}{\gamma})^2 \; W(\Delta)$$

Rate equations for cooling and heating

cooling:

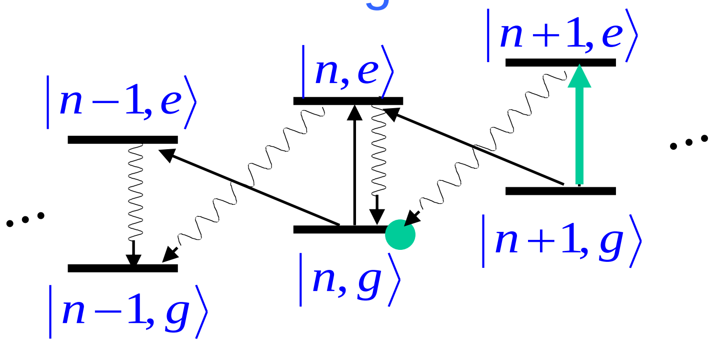

heating:

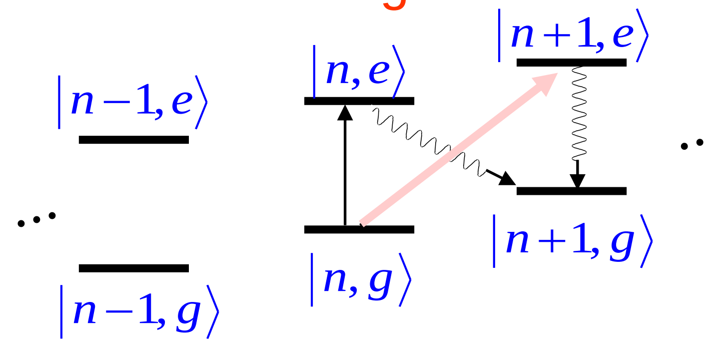

probability for population in |g,n>: loss and gain from states with |±n>

$$\dot{P}_{g,n} = \eta^2\gamma\left(\frac{\Omega}{\gamma}\right)^2 \cdot \left(\begin{array}{l|l} -nW(\Delta)P_n & -(n+1)W(\Delta)P_n \\ -nW(\Delta+\omega)P_n & \boxed{-(n+1)W(\Delta-\omega)P_n} \\ \hline \boxed{+(n+1)W(\Delta)P_{n+1}} & +nW(\Delta)P_{n-1} \\ +(n+1)W(\Delta+\omega)P_{n+1} & +nW(\Delta-\omega)P_{n-1} \end{array} \right) \begin{array}{l} \text{loss} \\ \\ \text{gain} \end{array}$$

cooling | heating

S. Stenholm, Rev. Mod. Phys. ***58***, *699 (1986)*

Rate equation

cooling:

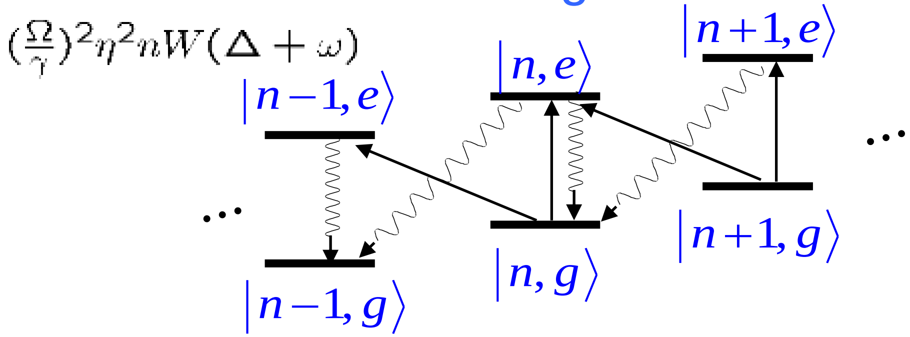

heating:

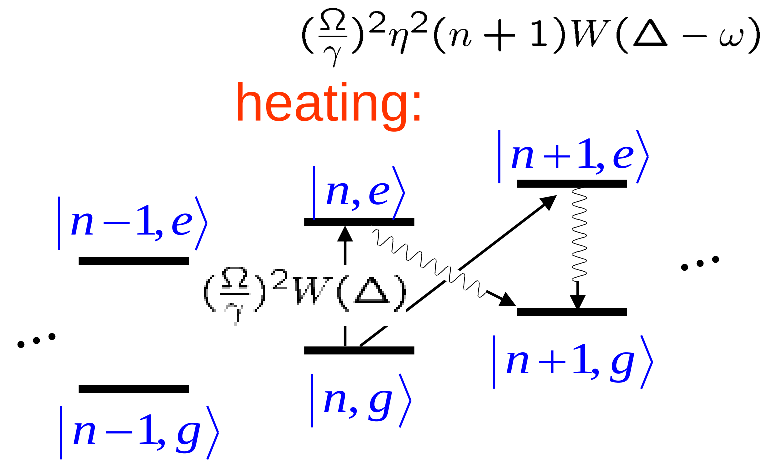

$$A_- = W(\Delta) + W(\Delta+\omega) \quad \text{cooling}$$

$$A_+ = W(\Delta) + W(\Delta-\omega) \quad \text{heating}$$

$$A_- - A_+ = W(\Delta+\omega) - W(\Delta-\omega)$$

different illustration:

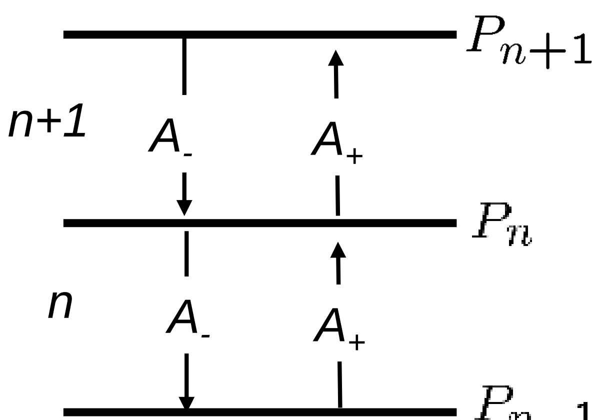

$$\langle \dot{n} \rangle = \frac{(\eta\Omega)^2}{\gamma} \sum n \frac{dP_n}{dt}$$

$$\Longrightarrow \quad \langle \dot{n} \rangle \sim -(A_- - A_+)\langle n \rangle + A_+$$

$$\langle n \rangle_{ss} = \frac{A_+}{A_- - A_+} \qquad 1/\tau_{cool} = \frac{(\eta\Omega)^2}{\gamma}(A_- - A_+)$$

steady state phonon number — cooling rate

How to reach $A_- > A_+ \Rightarrow W(\Delta+\omega) > W(\Delta-\omega) \Rightarrow$ red detuning $\Delta < 0$

„Weak confinement“

$$\boxed{\omega_{trap} << \gamma}$$

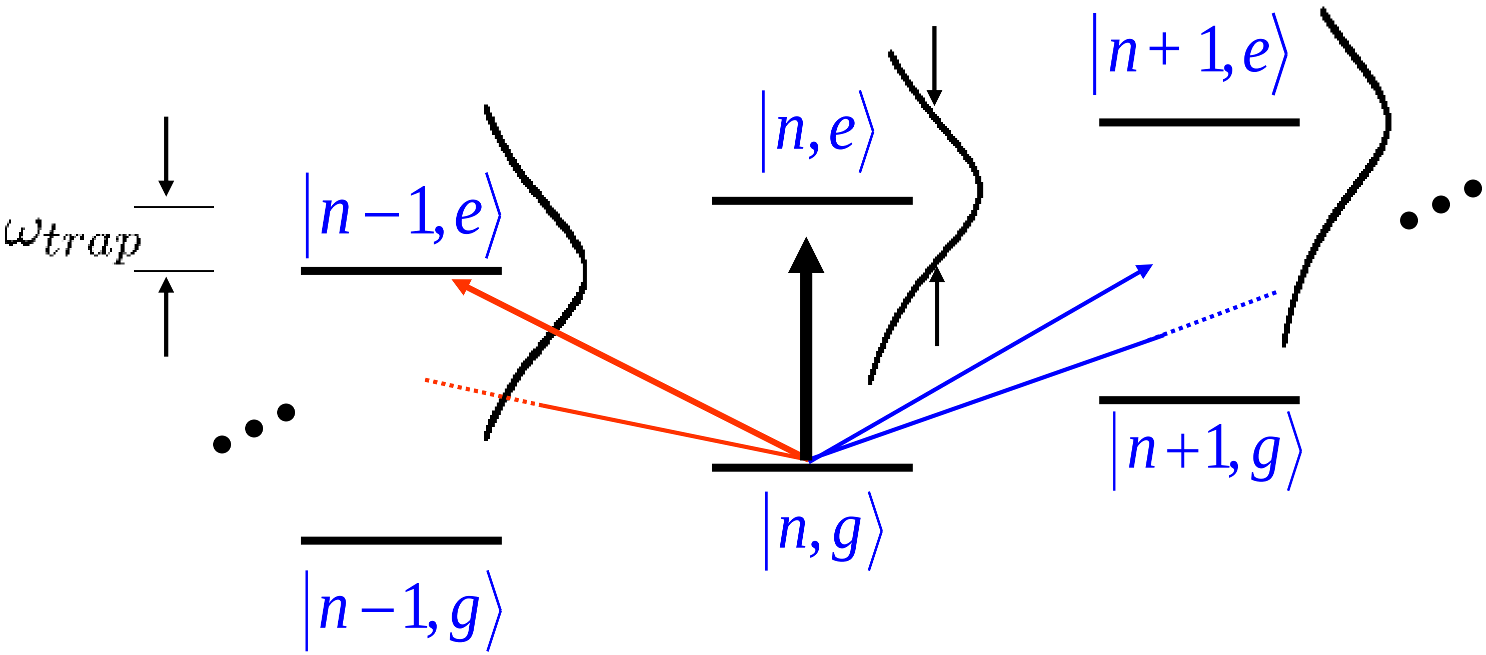

weak confinement:
Sidebands are not resolved on that transition.
Small differences in $W(\Delta \pm \omega), W(\Delta - \omega)$

$$\boxed{\text{detuning for optimum cooling } \Delta = -\gamma/2 \quad \Rightarrow \quad \langle n \rangle_{ss} = \frac{\gamma/2}{\omega_{trap}}}$$

„Weak confinement“

$$\boxed{\omega_{trap} << \gamma}$$

Lorentzian has the steepest slope at $-\gamma/2$

Doppler cooling

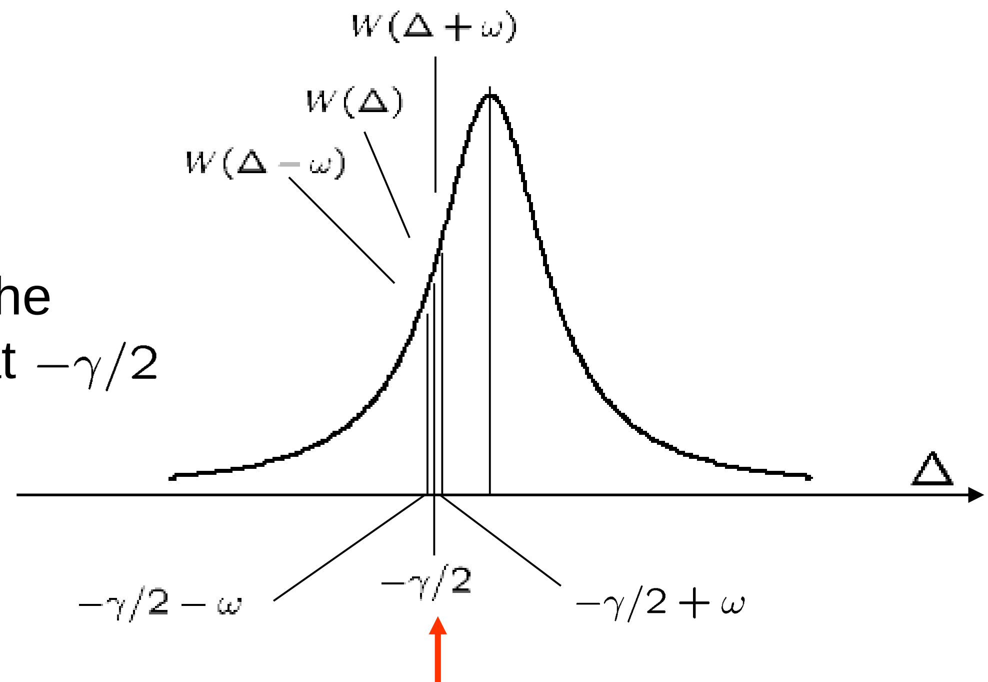

Laser

complications:

- $\eta_{laser} < \eta_{spontaneous}$
- saturation effects
- optical pumping
- multi-levels

weak confinement:
Sidebands are not resolved on that transition.
Small differences in $W(\Delta \pm \omega), W(\Delta - \omega)$

detuning for optimum cooling $\Delta = -\gamma/2 \quad \Rightarrow \quad \langle n \rangle_{ss} = \frac{\gamma/2}{\omega_{trap}}$

„Strong confinement“

$$\boxed{\omega_{trap} >> \gamma}$$

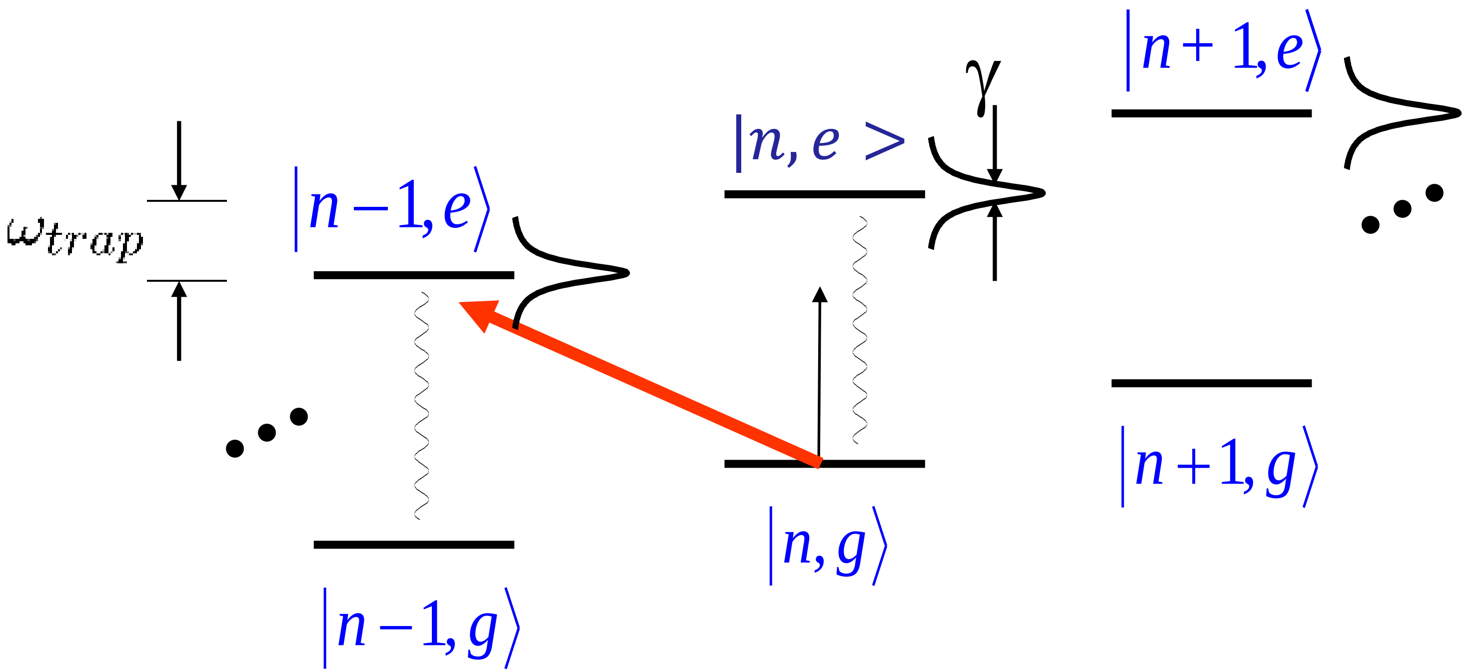

strong confinement – well resolved sidebands:
detuning for optimum cooling

$$\boxed{\Delta = -\omega_{trap} \quad \Rightarrow \quad \langle n \rangle_{ss} \approx (\frac{\gamma/2}{\omega_{trap}})^2 << 1}$$

„Strong confinement"

$$\boxed{\omega_{trap} >> \gamma}$$

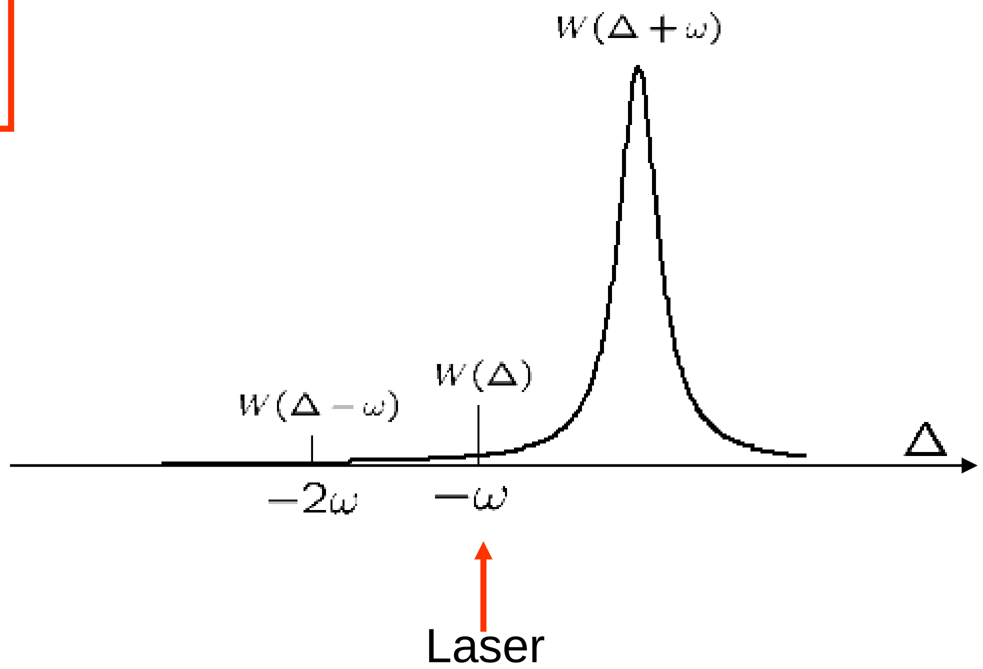

ground state cooling

strong confinement – well resolved sidebands:
detuning for optimum cooling

$$\boxed{\Delta = -\omega_{trap} \;\Rightarrow\; \langle n \rangle_{ss} \approx \left(\frac{\gamma/2}{\omega_{trap}}\right)^2 << 1}$$

Cooling limit

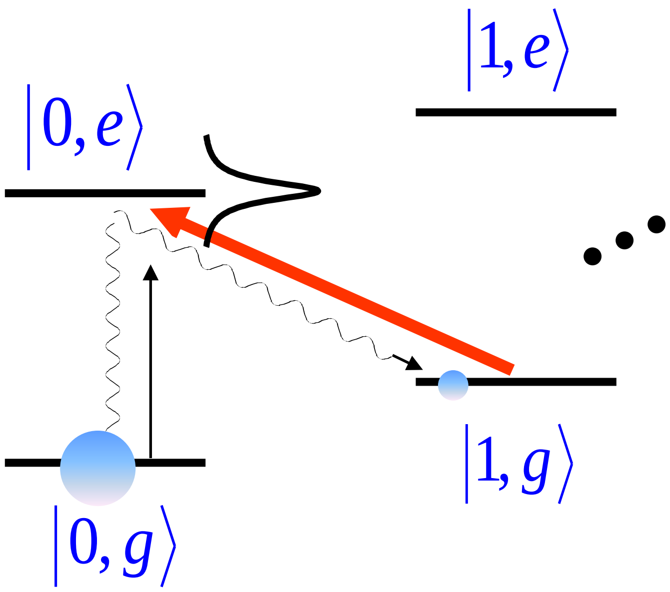

$$\Delta = -\omega_{trap}$$

Sideband ground state cooling

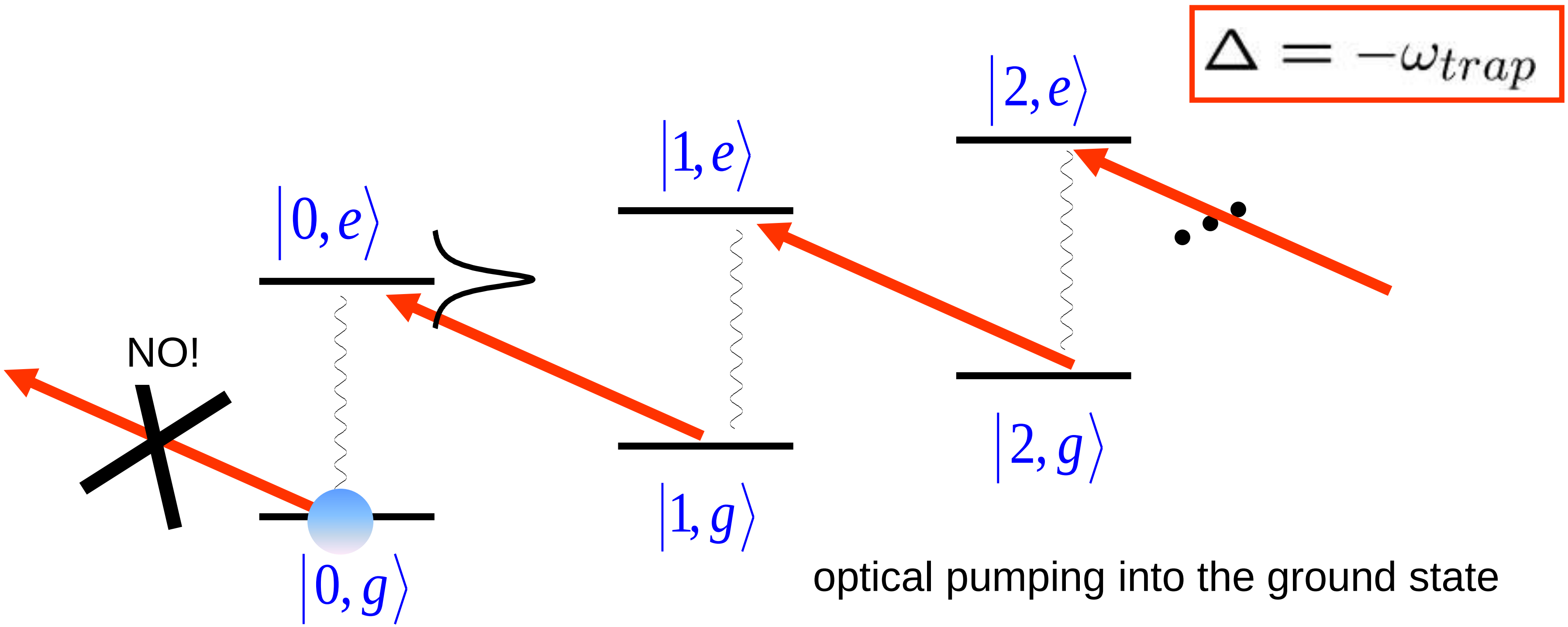

optical pumping into the ground state

Signature: no further excitation possible
„dark state" |0>

Temperature measurements

different methods

- observe Rabi oscillations on the blue SB
- compare the excitation on the blue SB and the red SB
- compare the excitation on the red SB and the carrier

Experimental: test excitation $P_e(t)$ for $\Delta=-\omega$ and $\Delta=+\omega$
Analysis: $P_{red}/P_{blue} = m\,/\,(m+1)$

$$P_e^{red}(t) = \sum_{n=1} \frac{m^n}{(m+1)^{n+1}} sin^2(2\pi\Omega_{n,n-1}t)$$

$$= \frac{m}{m+1} \sum_{n=0} \frac{m^n}{(m+1)^{n+1}} sin^2(2\pi\Omega_{n+1,n}t)$$

using: $\Omega_{n+1,n} = \Omega_{n,n+1}$

$$\Rightarrow \quad P_e^{red}(t) = \frac{m}{m+1} P_e^{blue}(t)$$

$$m = \frac{R}{1-R}, \quad R = P_e^{red}/P_e^{blue}$$

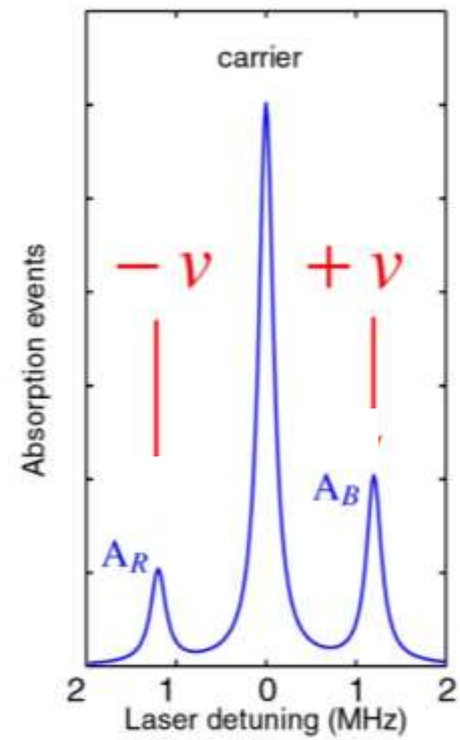

Example: ground state cooling

99.9% ground state population

$^{40}Ca^+$

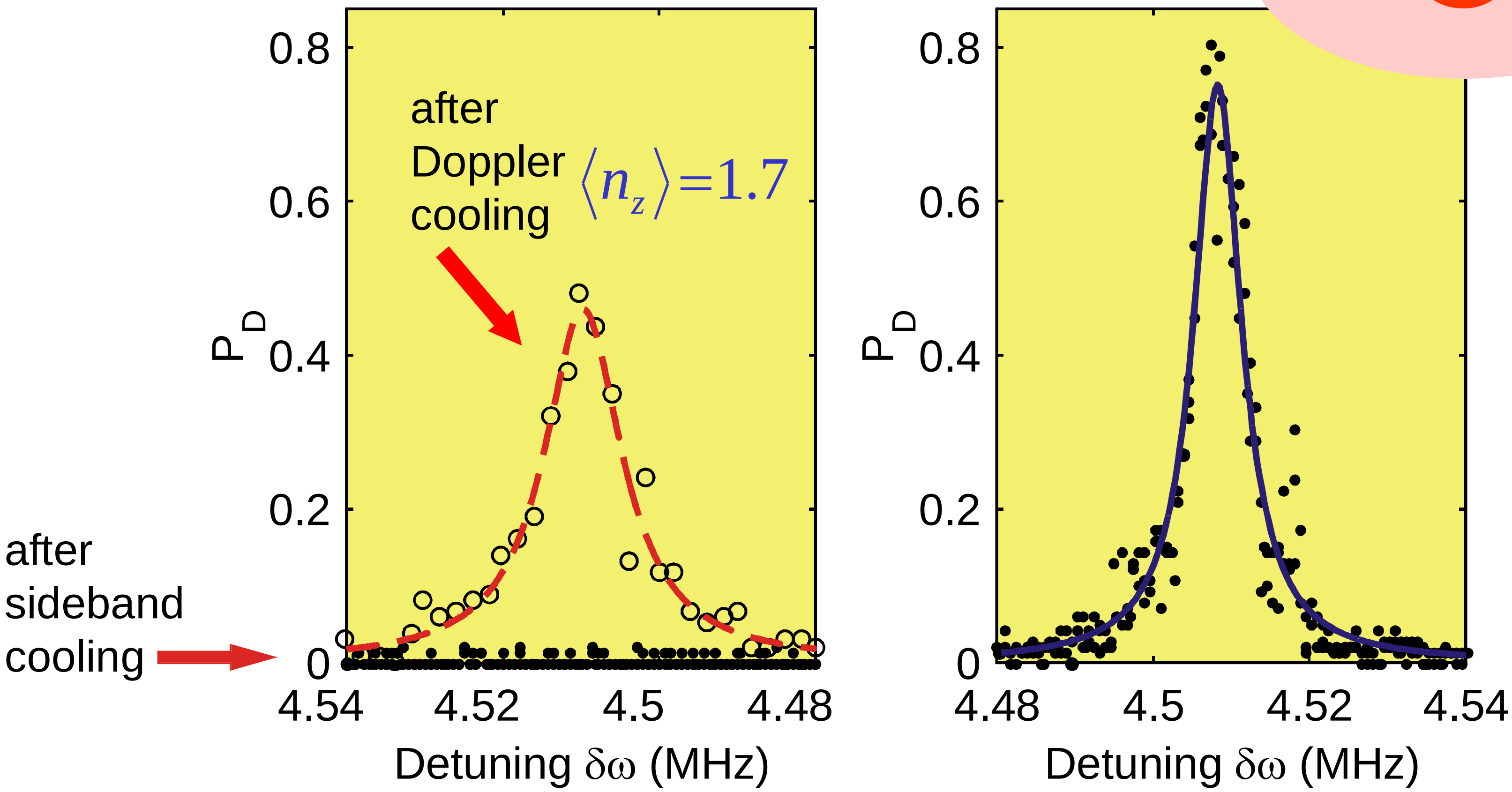

Ch. Roos et al., Phys. Rev. Lett. 83, 4713 (1999)

Simplifieds ion energy levels

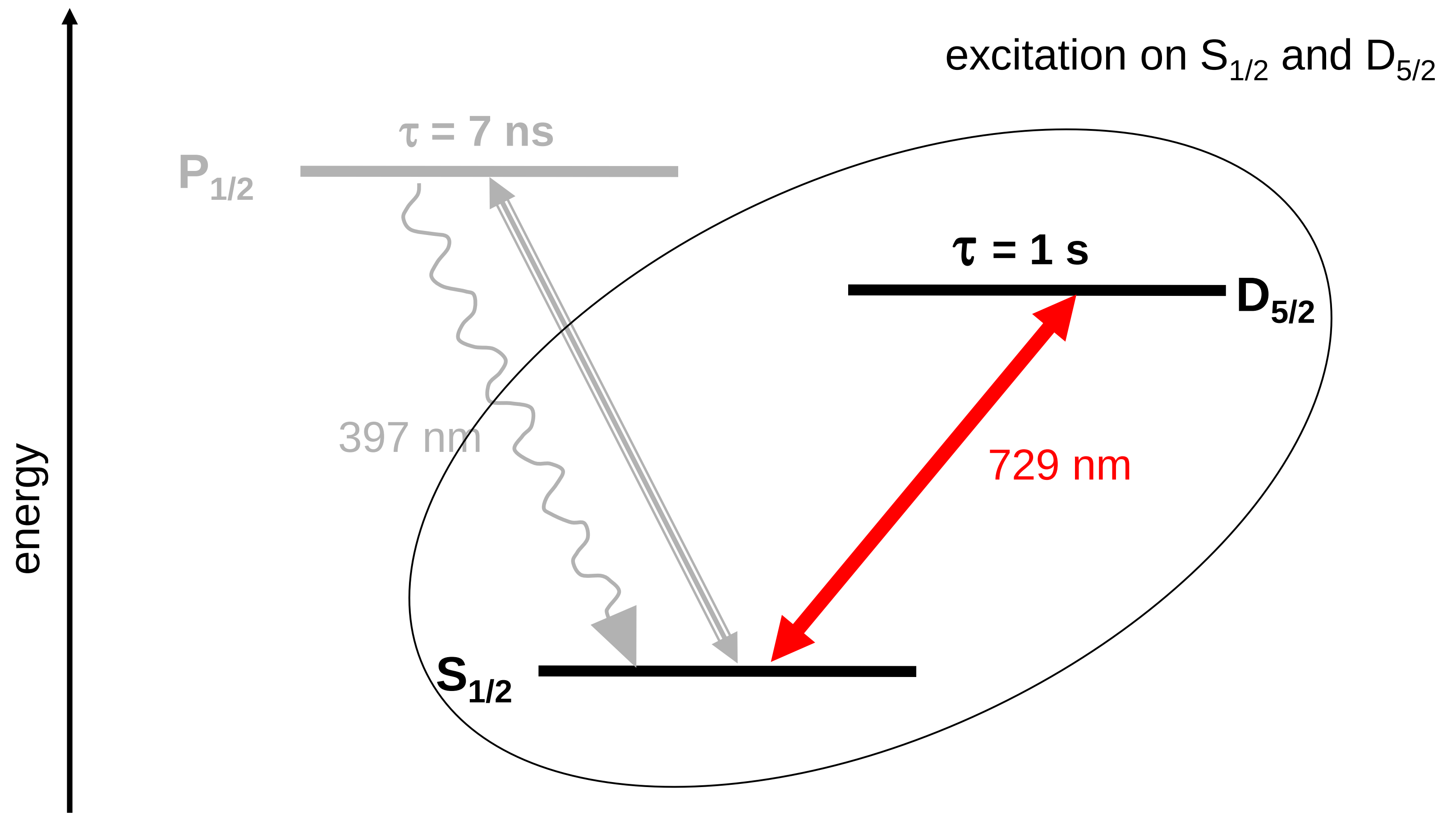

Simplifieds ion energy levels

Specroscopy pulse followed by detection:

Scatter light near 397nm:
$S_{1/2}$ emits fluorescence
$D_{5/2}$ remains dark

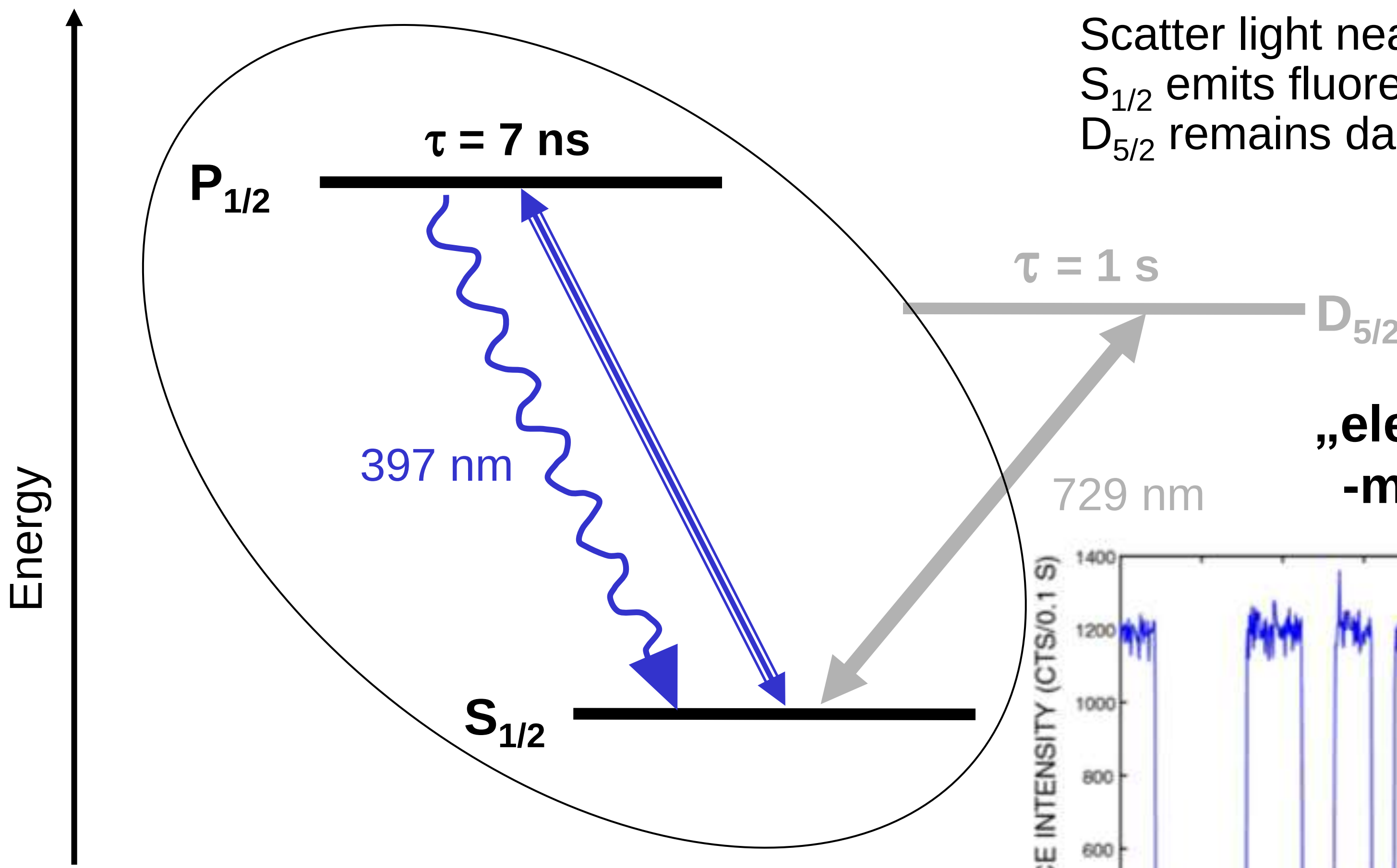

„electron shelving -measurement“

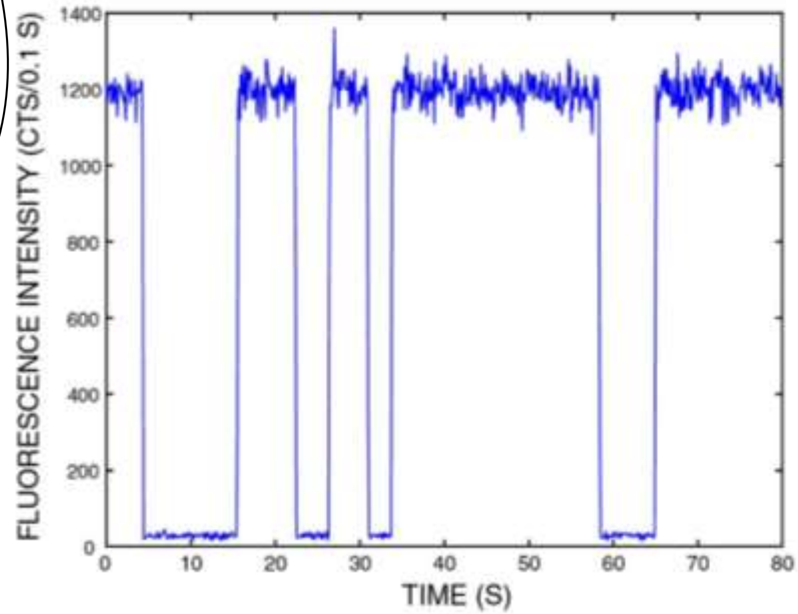

Resolved sideband spectroscopy

Select narrow optical transition with: $0.2..20MHz \sim \omega_{trap} >> \gamma$

a) Quadrupole transition
b) Raman transition between Hyperfine ground states
c) Raman transition between Zeeman ground states
d) Octopole transition
e) Intercombination line
f) RF or MW transitions

Species and Isotopes:

for (a)	^{40}Ca, ^{43}Ca, ^{138}Ba, ^{199}Hg, ^{88}Sr, ...
for (b)	^{9}Be, ^{43}Ca, ^{111}Cd, ^{25}Mg....
for (c)	^{40}Ca, ^{24}Mg, ...
for (d)	$^{172/172}$Yb, ...
for (e)	^{115}In, ^{27}Al, ...
for (f)	^{171}Yb, ...

Reminder to Doppler cooling

Advantage:
Cools all modes simultaneously

Problems:
But **not** into ground state
a) Sidebands are not resolved on the transition,
$\Rightarrow$ small differences in

$$W(\Delta \pm \omega), W(\Delta - \omega)$$

b) Carrier excitation leads to diffusion, $\Rightarrow$ heating:

$$W(\Delta = 0) \neq 0$$

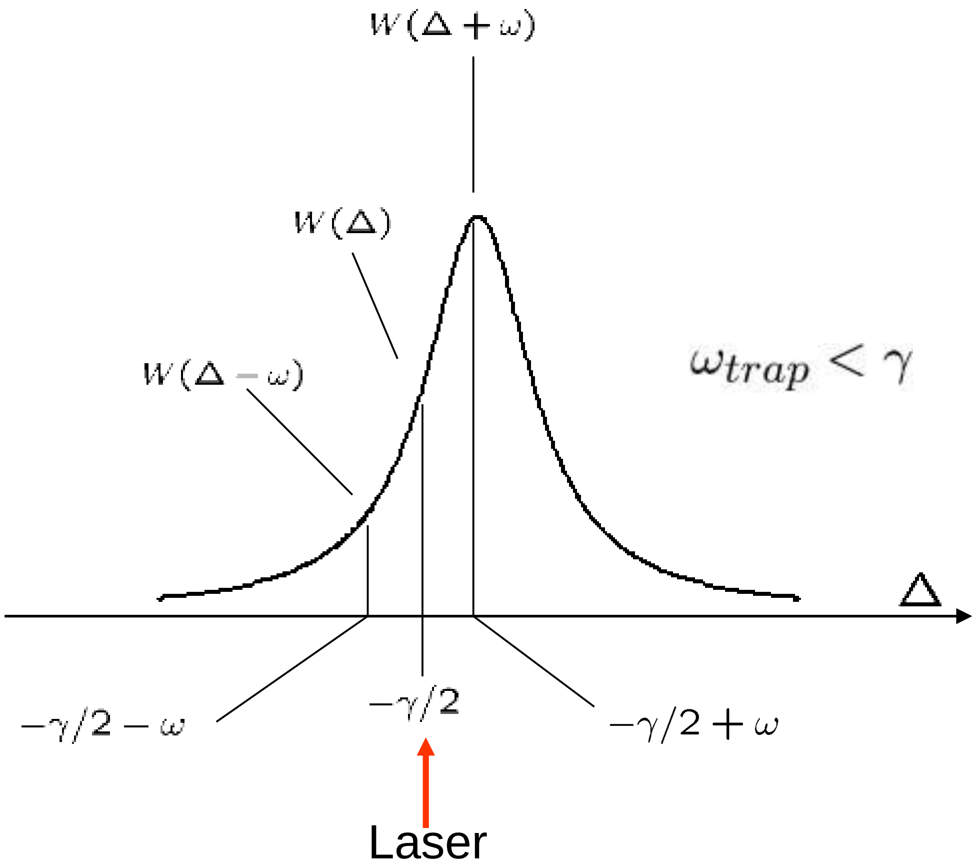

How to shape the atomic resonance line? $\Rightarrow$ **Quantum-Interference**

Dark resonance: $|\Psi\rangle = \frac{1}{\sqrt{2}}\left(|S_{1/2}\rangle - |D_{5/2}\rangle\right)$

$\Rightarrow$ spectrally much sharper than Dopper profile

Quantum interference and dark states

$$\Omega^{blue}_{Rabi} = 0.5 MHz$$
$$\Omega^{red}_{Rabi} = 20 MHz$$

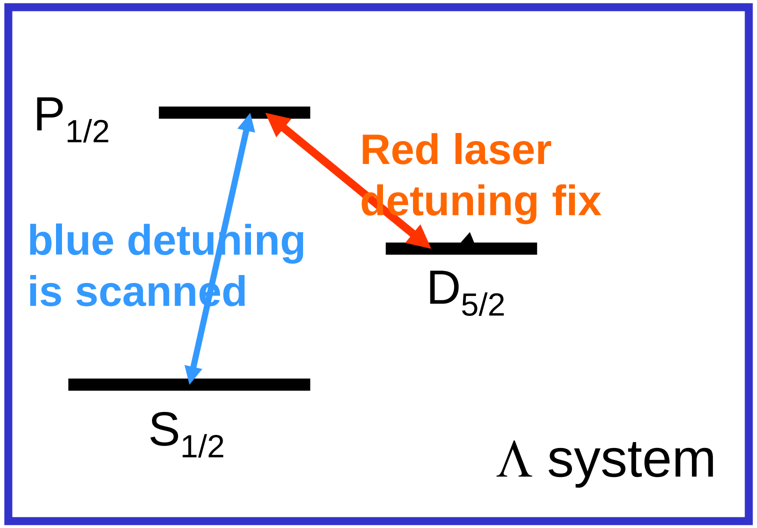

Shape of $W(\Delta)$ is no longer Lorentzian

Δ = 0

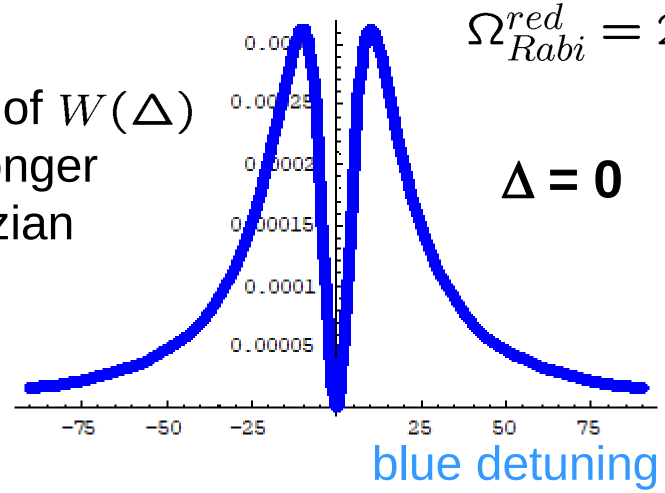

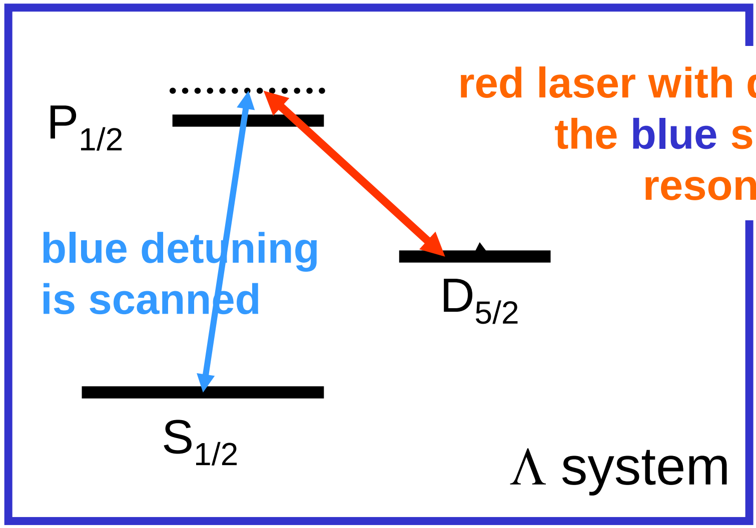

red laser with detuning fix to the blue side of the resonance

Δ = + 55MHz

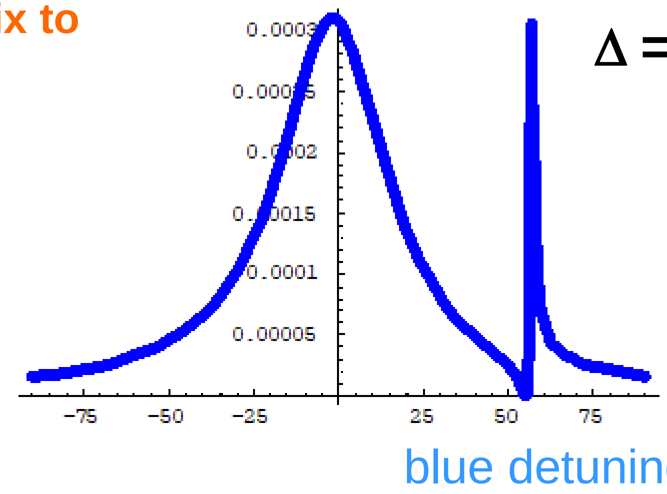

Ground state cooling with quantum interference

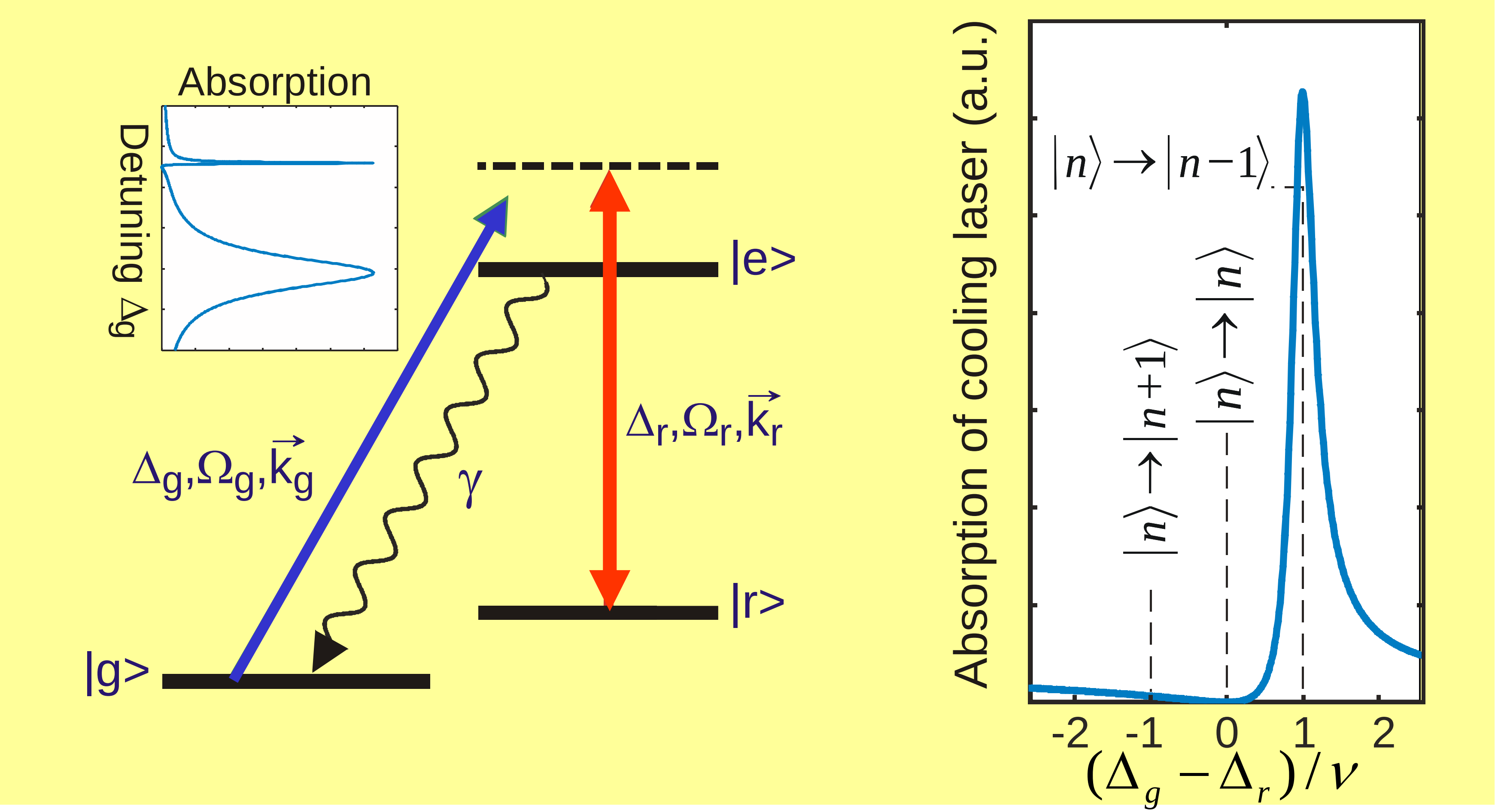

$|n\rangle \to |n-1\rangle$ transitions are enhanced by bright resonance

$|n\rangle \to |n\rangle$ transitions are suppressed by quantum interference – no „carrier“ diffusion contribution !

G. Morigi, J. Eschner, C. Keitel, Phys. Rev. Lett. 85, 4458 (2000)

Simultaneous two mode ground state cooling

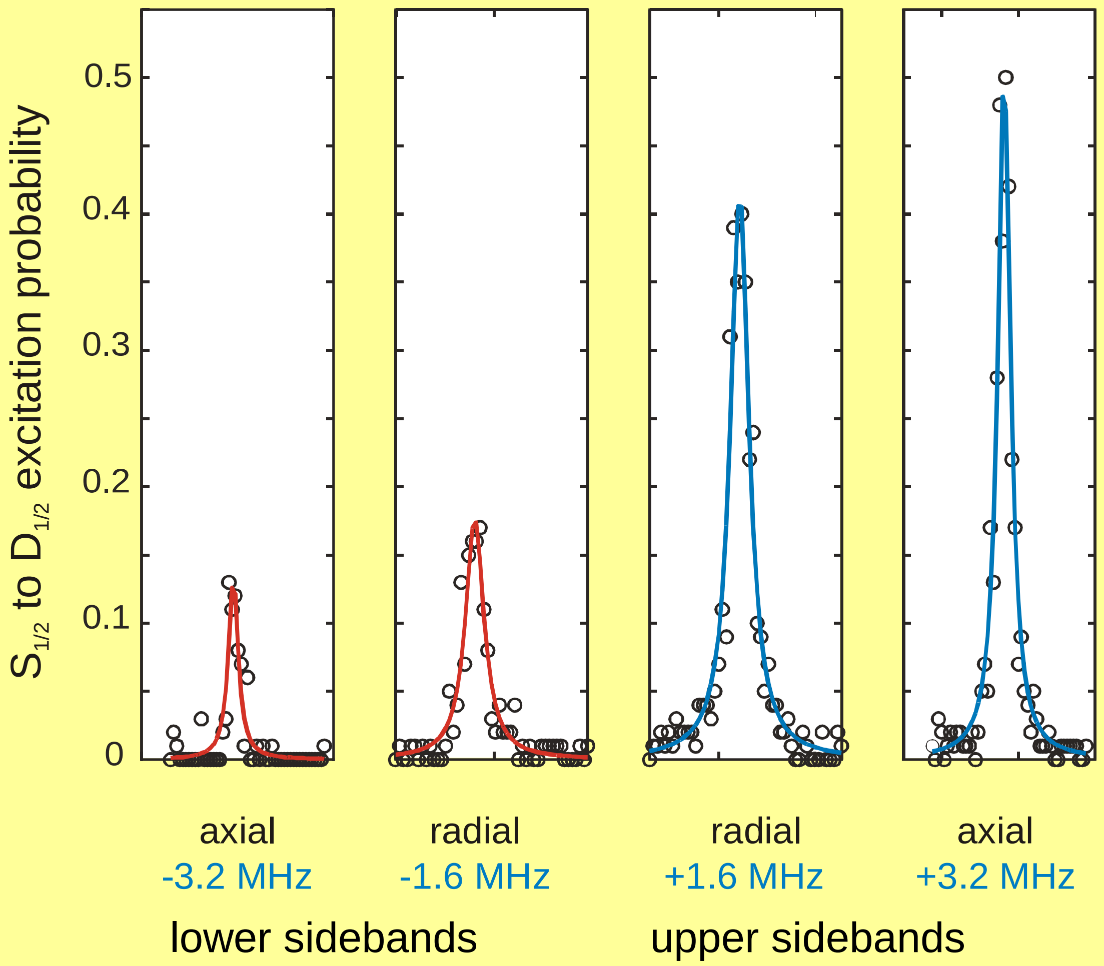

Simultaneous ground state cooling of axial and radial motion

axial:
P(0)=73%

radial:
P(0)=58%

Roos et al., Phys. Rev. Lett. 85, 5547 (2000)

Multi-mode ground state cooling

Simultaneous ground state cooling of **18 axial modes** to n~ 0.01..0.02

Lechner et al, PRA 93, 053401 (2016)

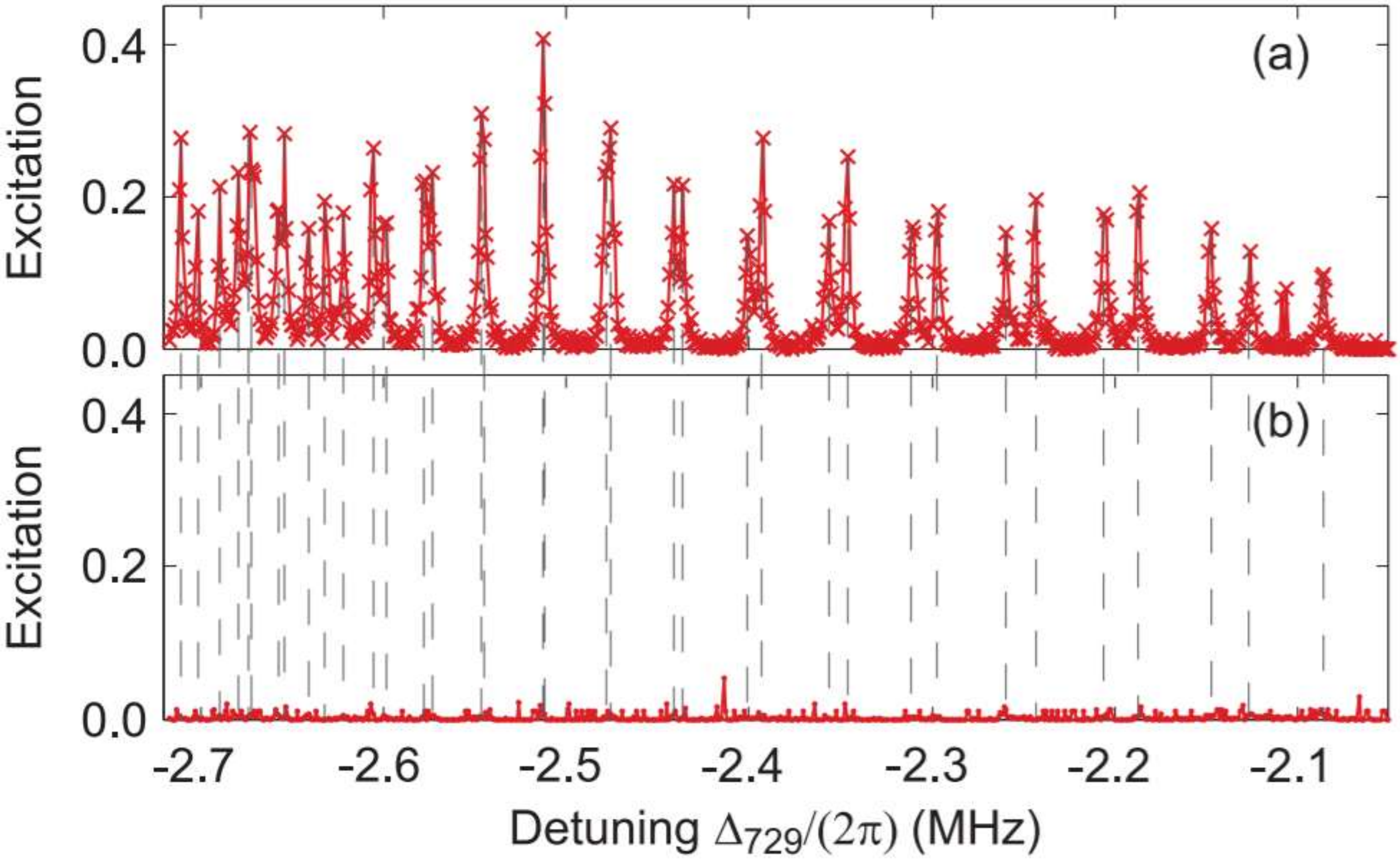

Quantum quantum information and thermodynamics with ions

- Introduction to ion trapping and cooling
- Trapped ions as qubits for quantum computing and simulation
- Qubit architectures for scalable entanglement
- Quantum thermodynamics introduction
- Heat transport, Fluctuation theorems,
- Phase transitions, Heat engines
- Outlook

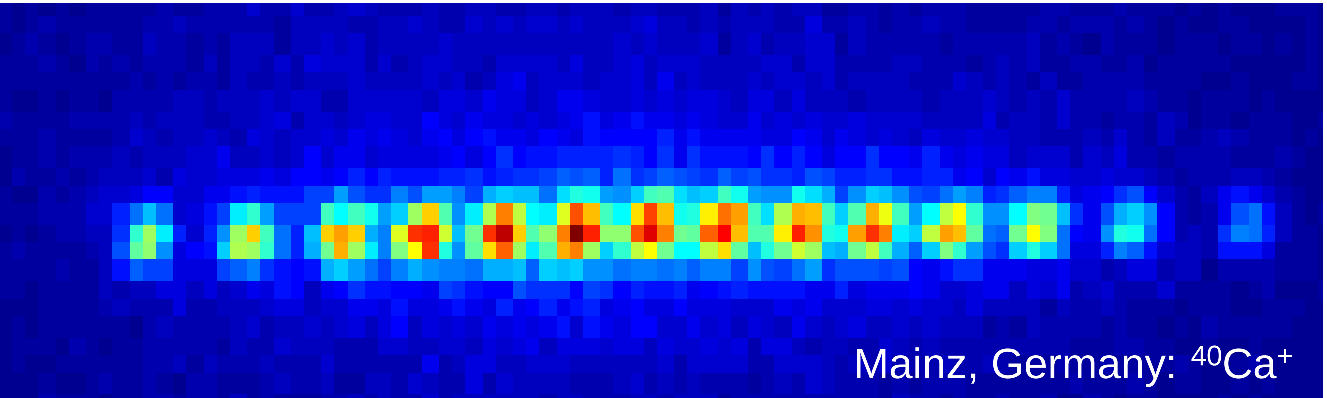

www.quantenbit.de

F. Schmidt-Kaler

JOHANNES GUTENBERG UNIVERSITÄT MAINZ